May 2024

Dark Matter From 2-Flavour Strongly Coupled Gauge Theory

Roberts Fišers

Theoretical Particle Physics
Division of Particle and Nuclear Physics
Department of Physics
Lund University

Master thesis (30 hp) supervised by Roman Pasechnik

LUND
UNIVERSITY

Abstract

Potential Dark Matter from strongly coupled gauge theory has been studied extensively in the past. However, in studies thus far, the combination of the phenomenological glueball state with the Linear sigma Model has yet to be explored. We provide the basis for a theory containing both the glueball and the sigma meson coupled to the Polyakov loop. Through considering only the lightest meson states and assuming classical field evolution we explore the cosmological evolution of the glueball and sigma fields. Our findings suggest that in such a theory the sigma meson is always heavier than the glueball, but the characteristics of the cosmological evolution of the fields is independent of the mass difference, which is rather dependent on the parameter choice.

Populärvetenskaplig beskrivning

Since the first experimental suggestions of presence of matter invisible to the human eye back in the 1930s, dark matter has been a captivating question both in the science community and in popular media. In the 1970s, through investigating the rotation of stars around the centre of the galaxy, we gained confirmation of the presence of dark matter in not only other galaxies, but also our very own Milky Way galaxy, and set the stage for investigating its distribution withing a galactic plane. Further, current theoretical and experimental developments suggest that there is five times as much dark matter as there is visible matter in the Universe, all of which possibly only interacts with visible matter through the gravitational force. The presence of dark matter is crucial for the evolution of the Universe, as it played an important role in early galaxy formation, and in the present epoch is responsible not only for the rotational trajectories of stars, but also for formation of galactic clusters.

While our understanding of dark matter and its importance in the contexts of the evolving Universe has grown drastically over the years, we still lack a clear-cut answer to questions, such as, what exactly it is on a fundamental level, what is its origin and why is there so much more dark matter than visible matter? In this work we set out to explore a potential candidate for light dark matter particles formed during the early evolution of the Universe. One of our candidates is the hypothetical glueball state, which is formed from the strong force mediators - gluons. The glueball forms during the confinement phase transition, which is the same phase transition where quarks come together to form composite states, we know as hadrons. The independent basis theory for our work has been well explored in previous research, and we seek to combine the well-established models into one combined model. We then investigate the cosmological evolution of our potential dark matter particles and the associated energy density of the condensate.

Contents

List of acronyms

SM - Standard Model

DM - Dark Matter

VEV - Vacuum Expectation Value

LσM - Linear Sigma Model

FLRW - Friedmann-Lemaitre-Robertson-Walker

QCD - Quantum Chromodynamics

YM - Yang-Mills

List of Figures

List of Tables

1 Introduction

The concept of dark matter (DM) has been captivating scientists ever since a "missing mass problem" was proposed from experimental observations of dynamics of stars in the Milky Way by J. Kapteyn in 1922 [1]. Further notable studies suggesting the existence of non-luminous matter in the Universe were conducted by F. Zwicky [2] in the 1930s, who studied the Coma cluster, and by V. Rubin during 1970s [3], who investigated the rotation curve of stars in the Milky Way. While today we understand the importance of DM in the context of the evolving Universe, we are yet to define it on a fundamental level, and understand its exact formation and evolution associated with its dynamics. One of the ways of investigating DM, which has shown promising signs, has been in the strongly coupled regime. Particularly, through the use of models which decouple from the Standard model of particle physics in the early stages of the evolving Universe.

Recent work on DM arising from the strongly coupled gauge theory, commonly referred to also as Yang-Mills theory, has made use of two well established models: the Linear sigma model (LσM) and the glueball. Particularly, Refs. [4] and [5] focused on exploring light DM in the form of a theoretical colour singlet state known as the glueball combined with the Polyakov loop, for a generic $SU(N)$ gauge theory. Here the glueball emerged through an associated confinement-deconfinement phase transition. The investigation was done over a parameter space spanned by the confinement scale and temperature ratio between the visible and dark sectors. The region corresponding to a scenario where the glueballs can account for the totality of DM was identified, indicating the glueball as a good a potential candidate for cold DM. Meanwhile Ref. [6] investigated the LσM for 3 quark flavours in low-energy Quantum Chromodynamics (QCD). Specific focus was laid on thermal evolution of thermodynamic observables, such as, pressure, entropy and energy density in the meson plasma. Thermal evolution of the lightest meson masses and the dynamics surrounding the associated symmetry breaking phase transition was also investigated. On the other hand, Ref. [7] employed the LσM in combination with the Polyakov loop, known as the Polyakov loop improved Linear sigma model (PLσM). Using this model they studied the first-order phase transitions and the accompanying gravitational wave signature. However, a combination of all three of the models: the glueball and the LσM coupled to the Polyakov loop, and the resulting consequences on the cosmological evolution of the underlying dynamics has not yet been explored in the literature.

We seek to investigate light DM particles arising from the strongly-coupled gauge theory in the case of two quark flavours, the up- and the down-quark. We focus on the $SU(3)$ gauge group and consider the glueball and the LσM to be coupled to the Polyakov loop. To this end, our investigation consists of two parts. Firstly, we extend the analysis carried out in Refs. [4] and [5] with the inclusion of the LσM. We treat the glueball and the sigma field as homogeneous classical fields evolving in the Friedmann-Lemaitre-Robertson-Walker metric. Secondly, we introduce a starting point for effective quantum field theory

(QFT) approach to finite temperature dynamics of the theory using of the generating functional method. The generating functional method is particularly useful for deriving the cosmological evolution of the thermodynamic observables describing the meson gas at finite temperature.

The structure of this thesis work is as follows. We begin by shortly introducing the theoretical basis for our study in section 2. Here we provide a brief overview of the symmetry breaking and associated phase transition concepts present when considering the glueball and the LσM coupled to the Polyakov loop. Section 3 lays out our model in its full detail. First we discuss the glueball, the Polyakov loop and the LσM in sections 3.1, 3.2 and 3.3 respectively from a general point of view. Then we construct the effective Lagrangian of our theory in section 3.4. Section 4 focuses on presenting the theory necessary for investigating the cosmological evolution of our theory in the classical regime. Results of this analysis are presented in section 5. Section 6 covers our progress in the QFT treatment, where we aimed to derive the thermal evolution of thermodynamic observables describing the condensate. Lastly, we present our main conclusions and outlook for potential future studies in section 7.

2 Theoretical Background

In this section we aim to lay the theoretical foundation for the study of DM particles arising from strongly coupled gauge theory. We begin by briefly summarizing some of the main aspects of Yang-Mills theory and explore the physics of chiral symmetry breaking. In the second half of the section we discuss the physics of phase transitions.

2.1 Yang-Mills Theory

Yang-Mills (YM) theory is a non-Abelian, strongly coupled QFT, which is built upon the mathematical structure of Lie groups. It describes interacting spin 1 fields and is the main theory used to describe the weak and the strong forces within the Standard Model. QCD is a specific realization of the YM theory in the context of the Lie group $SU(3)$, while for the Lie group $U(1)$ the YM theory reduces to the Maxwell theory.

A key point of study in the YM theory is the action S and the Lagrangian $\mathcal{L}$. In the case of QCD, the Lagrangian may be defined as

$$\mathcal{L}_{\text{QCD}} = -\frac{1}{4}G^{\mu\nu}G_{\mu\nu} + \sum_{i=1}^{N_f} \bar{\psi}_i(i\gamma^\mu \mathcal{D}_\mu - m_f)\psi_i, \tag{2.1}$$

where $G^{\mu\nu}$ is the gluon field strength tensor and the sum runs over the fermionic degrees of freedom, $\mathcal{D}_\mu = I\partial_\mu - igA^a_\mu T_a$ the covariant derivative with I the unit matrix, T_a the $SU(3)$ generators, A_μ the gauge field and g the coupling constant. The value of the coupling constant g distinguishes between strongly coupled and weakly coupled theories. Particularly, the limit $g \longrightarrow 0$ implies the weakly coupled regime, while $g \longrightarrow \infty$ implies the strongly coupled limit. The dynamical properties of the fields in the YM theory are studied by invoking the stationary-action principle, which in the Lagrangian formalism gives rise to the well-known Euler-Lagrange equation [8]. The non-Abelian nature of the YM theory introduces non-linear terms in the equations of motion. The presence of these terms implies that fields in YM theory are self-interacting. The self-interactions between the fields are responsible for giving rise to a phenomenon known as confinement. Lastly, interactions amongst the fields in the theory are introduced due to gauge invariance.

2.2 Chiral Symmetry Breaking

Chiral symmetry and confinement are two cornerstone phenomena in the YM theory. Chiral symmetry breaking is associated with the dynamics of quarks and contributes to their physical mass. According to the Goldstones theorem, the consequence of breaking chiral symmetry is production of Goldstone bosons [8]. Confinement, on the other hand, is responsible for the formation of massive composite states of particles, and the phenomenological fact that there are no isolated quarks. If sufficient energy is input in the system to

overcome the strong attractive force, a virtual quark-antiquark pair would be created. The physics of such events are described by the well-know Lund model [9]. While establishing the theoretical foundations of confinement is quite complex and beyond this paper, chiral symmetry breaking may be presented in a more straightforward manner. In this section we briefly introduce the theoretical formalism associated with chiral symmetry breaking following the methodology in Ref. [8].

The summation over fermionic degrees of freedom in equation (2.1) may be decomposed into left- and right-handed chirality parts as

$$\sum_{i=1}^{N_f} i\psi_{+i}^{\dagger}\bar{\sigma}^{\mu}\psi_{+i} + i\psi_{-i}^{\dagger}\sigma^{\mu}\mathcal{D}_{\mu}\psi_{-i}. \tag{2.2}$$

As a result, the classical Lagrangian has underlying symmetry of the form

$$G_F = U(N_f)_L \times U(N_f)_R \tag{2.3}$$

acting as $U(N_f)_L : \psi_{-i} \to L_{ij}\psi_{-j}$ and $U(N_f)_R : \psi_{+i} \to R_{ij}\psi_{+j}$ with L and R representing $N_f \times N_f$ unitary matrices.

Further decomposition in the underlying symmetry components yields that under the global $U(1)_V$ symmetry both ψ_- and ψ_+ transform in the same way as $\psi_{\pm,i} \to e^{i\alpha}\psi_{\pm,i}$. After chiral symmetry breaking the $U(1)_V$ symmetry is retained, and in the context of QCD it is referred to as the baryon number. On the other hand, under the axial symmetry $U(1)_A$, the left and right-handed fermions transform with an opposite phase: $\psi_{\pm,i} \to e^{\pm i\beta}\psi_{\pm,i}$. The presence of a phase shift between the left- and the right-handed fermions is responsible for introducing the so-called axial anomaly into the theory, commonly also referred to as the chiral anomaly.

As a result of the above two observations the global symmetry of the quantum theory is

$$G_F = U(1)_V \times SU(N_f)_L \times SU(N_f)_R. \tag{2.4}$$

The dynamics of the theory depend on the number of quark flavours N_f and the number of quark colours N_c. For low N_f the two main phenomena describing the low-energy physics of the model are confinement and quark condensate (chiral condensate). The quark condensate is the vacuum expectation value (VEV) of the composite operators $\psi_{+j}(x)\bar{\psi}_{-i}(x)$, and in strong coupling dynamics of non-Abelian gauge theories takes the form of

$$\langle\bar{\psi}_{-i}\psi_{+j}\rangle = -\tau\delta_{ij}, \tag{2.5}$$

with τ being a constant with dimension of $[\text{mass}]^3$. The formation of quark condensate is only possible within the strongly coupled regime because in weakly coupled theories chiral symmetry breaking does not take place.

The ground state of the chiral condensate is not invariant and transforms as $\langle\, \bar{\psi}_{-i}\, \psi_{+j}\, \rangle \;\rightarrow\; \tau\, (L^{\dagger} R)_{ij}$. This is an example of spontaneous symmetry breaking, and the condensate remains invariant only in the case of $L = R$. Meaning, the spontaneous chiral symmetry breaking may be described as

$$G_F = U(1)_V \times SU(N_f)_L \times SU(N_f)_R \rightarrow U(1)_V \times SU(N_f)_V, \tag{2.6}$$

with $SU(N_f)_V$ denoting the diagonal subgroup of $SU(N_f)_L \times SU(N_f)_R$. According to the Goldstone theorem the spontaneous symmetry breaking is associated with generation of mass-less particles known as Goldstone bosons. The number of such particles is equal to the number of broken generators, i.e. $N_f^2 - 1$.

For the two quark flavour case $N_f = 2$ considered in this study, the associated Goldstone bosons of chiral symmetry breaking are the pions. In fact, pions are pseudo-Goldstone bosons, because they have physical mass. They acquire their mass from explicit chiral symmetry breaking caused by bare quark masses. Per the Gell-Mann-Oaks-Renner relation [10] at zero temperature the pion mass can be expressed in terms of the $u\bar{u}$ and $d\bar{d}$ condensates and the pion decay constant f_π^2 as

$$m^2_{\pi(\mathrm{vac})} = -\frac{(m_u + m_d)\langle 0|\bar{u}u + \bar{d}d|0\rangle}{f_\pi^2}, \tag{2.7}$$

with the pion decay constant given as $f_\pi^2 \approx (130\ \mathrm{MeV})^2$ [11]. The pion decay constant f_π is also related to the breaking of the chiral symmetry. As a result, one may link f_π to the zero-temperature QCD order parameter v_0 as $f_\pi \equiv v_0/k_\pi$, with $k_\pi \approx 2$ [6]. Therefore, the zero-temperature pion mass may be rewritten as

$$m^2_{\pi(\mathrm{vac})} = 2\kappa(m_u + m_d)v_0^2, \tag{2.8}$$

$$\kappa = 4k_\pi^2 \left(\frac{9}{8}\Lambda_g + m_u + m_d\right)^{-1}, \tag{2.9}$$

where $m_u \approx 2.16$ MeV and $m_d \approx 4.70$ MeV [11] denote the constituent quark masses, and $\Lambda_g \approx 1.2$ GeV the gluon correlation length [12]. We will make use of this notation when defining the effective Lagrangian of our theory in section 3 and when investigating the generating functional method for deriving relations for observable thermodynamic variables of the condensate in section 6.

2.3 Phase transitions

Spontaneous symmetry breaking is commonly accompanied by a phase transition, where the condensate undergoes a transition from a local minimum in the potential to a lower energy global minimum. There are three main ways for a phase transition to occur: thermal excitation, where the energy necessary to overcome the potential barrier is obtained

from the medium, quantum tunnelling, when spontaneous tunnelling to the lower energy state take place, and thermally assisted tunnelling, where factors from both of the aforementioned possibilities contribute. A graphical representation of the three methods can be found in Figure 1. The nature of the phase transition is characterized in the following three ways. In a first-order phase transition a discontinuous change in one of more thermodynamic observables takes place and consequently latent heat is involved. A second-order phase transition is characterized by a continuous change in thermodynamic observable and no latent heat is involved. The third type is commonly referred to as a smooth crossover, where no critical behaviour may be noted. Hence, the presence of a first-order phase transition alongside the spontaneous symmetry breaking significantly impacts the dynamics of the associated fields and consequently the observable thermodynamic quantities describing the condensate.

In the context of an evolving Universe, thermally induced phase transition is the most probable scenario. In this case the evolution of the two minima in the potential may be described as follows. Initially the system resides in the lowest of the two minima (the global minimum) at equilibrium. At the critical temperature both minima have shifted such that they are equal. At this point, the fields may start to undergo thermally assisted transitions to the other minimum. As the temperature keeps decreasing the original global minimum becomes a local minimum, while the original local minimum becomes a global minimum and through thermal excitation the system transitions to the new global minimum. This concept may be extended to more than two minima, and new minima may also arise as the system evolves. [13]

Our study contains two phase transitions, which are associated with chiral symmetry breaking and confinement. Chiral symmetry breaking and confinement phase transitions are expected to occur at a similar energy scale [14]. The presence of a phase transition may have a noticeable impact on the evolution of the fields in the theory as well as on thermodynamic observables, such as pressure, energy density and entropy. In section 5 we consider the classical field theory perspective and focus on the thermal evolution of fields and the energy density of the condensate. While in section 6 we utilize the QFT approach to introduce the basis for deriving the impact of a phase transition on thermal evolution of the thermodynamic observables.

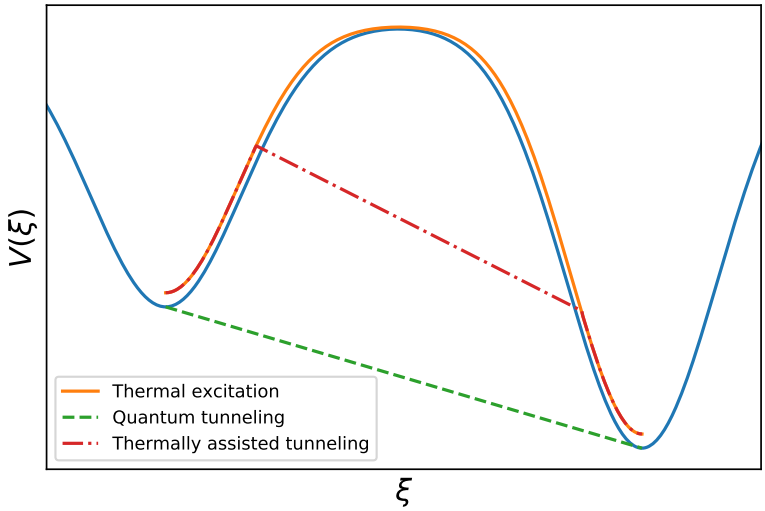

Figure 1: Representation of three ways a phase transition may occur in a medium. The potential is represented by the blue line. Orange, green, and red lines are graphical representations of the evolution in the potential the system undergoes during the phase transition.

3 THE EFFECTIVE LAGRANGIAN

In this section we introduce the main models and concepts considered in our approach of investigating formation and evolution of DM particles in Yang-Mills theory. Specifically, we introduce the glueball and outline the key concepts of the Polyakov loop and the LσM in a general way. We then combine these three ingredients to form the effective Lagrangian of our theory. Along the way, we explore how interactions between various parts arise, and present the basis for simplifications employed in our study.

3.1 The glueball

In the context of evolving Universe and quark-gluon plasma, glueballs are composite particles formed as a consequence of gluons confining during the confinement-deconfinement phase transition in a similar manner as mesons. The confining of gluons arises due to gluon self-interaction, which is mediated by the strong force. Same as mesons, the resulting confined state is a colour-singlet. Other physical properties of the glueball state are also very similar to those of ordinary mesons as outlined in Ref. [15].

In high-energy hadron collision experiments the glueball state is phenomenologically theorized as a scattering resonance state, with candidates such as the $f_0(1710)$ state. However,

at the moment of writhing this thesis, the glueball state is only a theoretical concept with no experimental confirmation. This is so most notably due to observational difficulties in scattering events, where the glueball state would mix with meson states [15], [16].

From the field theory perspective one chooses to associate the glueball dynamics with a dimension-4 field $\mathcal{H} \propto \mathrm{Tr}(G^{\mu\nu}G_{\mu\nu})$, with $G^{\mu\nu}$ being the QCD field strength tensor [4]. However, in the Lagrangian formalism we wish to associate the glueball with a dimension-1 field. Hence, we canonically normalize the glueball field $\mathcal{H}$ in the same manner as has been done in Ref. [4]. For this purpose, we make use of the redefinition $\mathcal{H} \propto 2^{-8}c^{-2}\phi^4$, where the parameter c is expressed as

$$c = (\Lambda/m_{\mathrm{gb}})^2/2\sqrt{e}, \tag{3.1}$$

with m_{gb} being the mass of the glueball in the confined phase, and Λ representing the confinement scale. We fix the value of the glueball mass to $m_{\mathrm{gb}} = 6\Lambda$ as per Ref. [17]. The relation between the critical temperature T_c of confinement-deconfinement phase transition and the confinement scale Λ will be presented in equation (3.7).

Then the Lagrangian density describing an evolving glueball field can be written according to Ref. [4] as

$$\mathcal{L}_{\mathrm{gb}} = \frac{1}{2}\partial_\mu\phi\partial^\mu\phi - V(\phi), \tag{3.2}$$

$$V(\phi) = \frac{\phi^4}{2^8c^2}\left(2\ln\left(\frac{\phi}{\Lambda}\right) - 4\ln 2 - \ln c\right). \tag{3.3}$$

Further on the properties of glueballs, modern developments in glueball spectroscopy and production and decays of glueballs in hadronic reactions can be found in [16].

3.2 Polyakov loop model

It is well established in the literature that fully gauge-invariant separation of phases must be associated with a first-order phase transition. According to the Elitzur's theorem [18], in such an event, breaking of a global symmetry must take place. In the case of a finite temperature T, the global symmetry of an $SU(N)$ gauge group is the centre symmetry $\mathbb{Z}_N$ [14], [19]. The centre symmetry is defined as a subset of elements within a gauge group, that commute with all elements of the given gauge group [14]. For $SU(N)$ gauge group the centre symmetry is the subgroup $\mathbb{Z}_N$: $\{\exp\big(2\pi in/(N\hat{1}_N)\big)\}$, where $n = 0, 1, ..., N-1$.

In QFT one often is interested in studying the effects of parallel transporting gauge invariant observables around closed loops. One such temperature dependent observable is the Polyakov loop. The Polyakov loop l is charged with respect to the aforementioned centre $\mathbb{Z}_N$ of the $SU(N)$ gauge group and transforms as $l \to zl$ with $z \in \mathbb{Z}_N$ [4]. The Polyakov

loop is defined as [20]

$$l(x) = \frac{1}{N}\,\mathrm{Tr}[\mathbf{L}] \equiv \frac{1}{N}\,\mathrm{Tr}\left(\mathcal{P}\exp\left[ig\int_0^{1/T} A_0(\tau,\mathbf{x})d\tau\right]\right), \tag{3.4}$$

where $\mathcal{P}$ is the path ordering, A_0 is the time component of the vector potential associated with a particular gauge group, $(\tau, \mathbf{x})$ are Euclidean spacetime coordinates and g is the $SU(N)$ coupling [4].

The Polyakov loop enters the Lagrangian of the theory through its potential term $V(l)$ and via interaction terms with other constituents present in the model (see section 3.4). In accordance with Ref. [20] the Polyakov loop potential $V(l)$ for an $SU(N)$ gauge group is defined as

$$V(l) = T^4\left(-\frac{b_2(T)}{2}|l|^2 + b_4|l|^4 - b_3(l^N + l^{*N}) + b_6|l|^6 + b_8|l|^8\right), \tag{3.5}$$

$$b_2(T) = a_0 + a_1\left(\frac{T_c}{T}\right) + a_2\left(\frac{T_c}{T}\right)^2 + a_3\left(\frac{T_c}{T}\right)^3 + a_4\left(\frac{T_c}{T}\right)^4, \tag{3.6}$$

$$T_c = \left(1.59 + \frac{1.22}{N^2}\right)\Lambda, \tag{3.7}$$

where the parameters of the potential a_i and b_i are determined from lattice simulations and their numerical values can be found in Table 1 as presented in Ref. [21]. The critical temperature T_c denotes the point of phase transition between the confined and deconfined phases of the quark-gluon plasma. Its dependence on the gauge group and the confinement scale Λ is also determined from lattice simulations [22], [23]. A graphical representation of the Polyakov loop potential in equation (3.5) in both the confined $T < T_c$ and the deconfined $T > T_c$ phases can be found in Figure 2. We display the potential for the gauge groups $N = 3, 4, 5$ as these have the most accurate and well agreed upon results from lattice simulations. The values used for the parameters in the plot can be found in Table 1. We note that while the shape of the potential, especially in the deconfined phase, is different between the gauge groups, the location of the minima in l in the potential is approximately the same. The obtained result is in exact agreement with the one displayed in Ref. [4].

An important property of the Polyakov loop is that its expectation value provides an order parameter for the confinement phase transition in the YM theory [4], which occurs at the energy scale Λ. This emerges through consideration of the expectation value of the Polyakov loop at different temperatures. Notably, at temperatures below T_c, the low-temperature limit, the expectation value of the Polyakov loop is zero, while at temperatures above T_c, the high-temperature limit, it is non-zero. The thermal evolution of the expectation value of the Polyakov loop for the gauge groups $N = 3, 4, 5$ can be seen in Figure 3. Again, we note that the difference in the evolution between the gauge groups is small, and

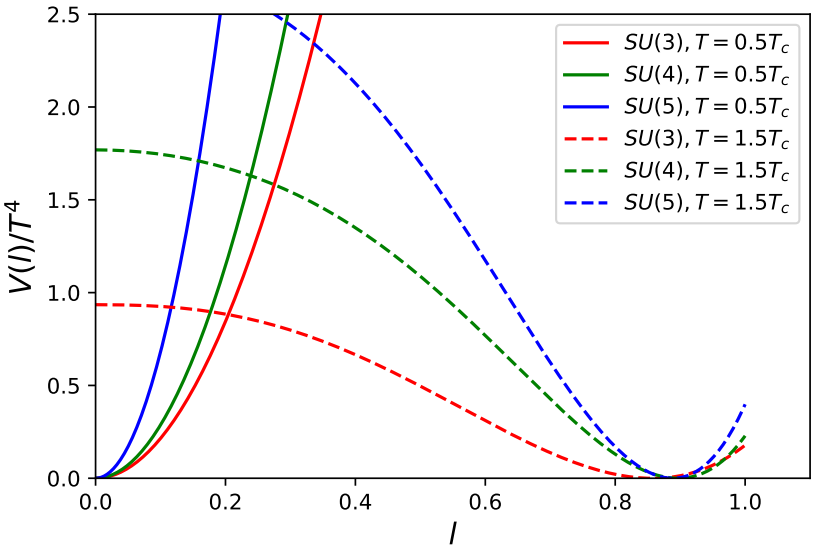

Figure 2: Polyakov loop potential as a function of the Polyakov loop l for $SU(N)$ gauge groups with $N = 3, 4, 5$ according to the equation (3.5). The values for parameters a_i and b_i are taken from lattice simulation in Ref. [21].

the obtained result agrees with the one presented in Ref. [4]. We will use this observation along the ones made from investigating the Polyakov loop potential in Figure 2 to limit our investigation to only the $SU(3)$ gauge group.

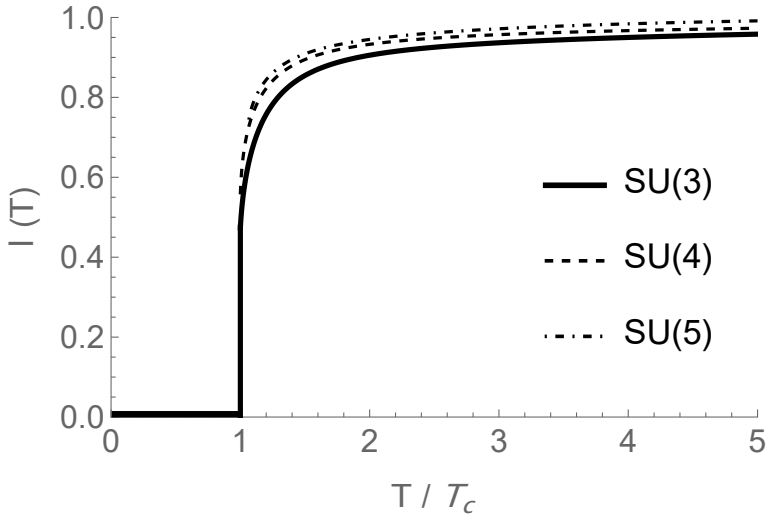

Figure 3: Thermal evolution of the expectation value of the Polyakov loop for gauge groups $N = 3, 4, 5$. The critical temperature T_c is defined according to equation (3.7).The values for parameters a_i and b_i entering the evolution are taken from lattice simulation in Ref. [21].

Table 1: Values of different parameters in Polyakov loop potential presented in equation (3.5) taken from lattice simulations in Ref. [21]

N	3	4	5
a_0	3.72	9.51	14.3
a_1	-5.73	-8.79	-14.2
a_2	8.49	10.1	6.40
a_3	-9.29	-12.2	1.74
a_4	0.27	0.489	-10.1
b_3	2.40	-	-5.61
b_4	4.53	-2.46	-10.5
b_6	-	3.23	-

3.3 Linear sigma model

The third major ingredient in our study of DM from strongly coupled gauge theory is the LσM, which realises the chiral symmetry breaking. Additionally, it introduces mesons in the system and is invariant under the global chiral $SU(N_f) \times SU(N_f)$ symmetry [24]. In the most general description, the LσM Lagrangian contains two Lorentz scalar fields: σ and a_a, and their associated chiral partners the Lorentz pseudo scalar fields η' and π_a. The LσM also captures the coupling of the mesons to the temporal background gauge fields through the covariant derivative.

The Lagrangian of the LσM containing the aforementioned fields and mesons coupling to a spatially constant temporal background is given as

$$\mathcal{L}_{\mathrm{L}\sigma\mathrm{M}} = \frac{1}{2}\partial_\mu\sigma\partial^\mu\sigma + \frac{1}{2}\partial_\mu\pi_a\partial^\mu\pi_a + V_{\mathrm{L}\sigma\mathrm{M}}, \tag{3.8}$$

where $V_{\mathrm{L}\sigma\mathrm{M}}$ is the potential of the LσM, q and $\bar{q}$ represent fermion fields and T^a are the generators of the appropriate $U(N_f)$ group. The general form of the potential for N_f number of quark flavours is given as

$$\begin{aligned} V_{\mathrm{L}\sigma\mathrm{M}} = {} & \bar{q}(i\partial - g(\sigma + i\gamma_5 T^a\pi_a))q + \frac{1}{2}(\lambda'_\sigma - \lambda_a)\,\mathrm{Tr}\big(\Phi^\dagger\Phi\big)^2 + \\ & \frac{N_f}{2}\lambda_a\,\mathrm{Tr}\big(\Phi^\dagger\Phi\Phi^\dagger\Phi\big) - m^2\,\mathrm{Tr}\big(\Phi^\dagger\Phi\big) - 2\alpha(2N_f)^{N_f/2-2}(\det\Phi^\dagger + \det\Phi), \end{aligned} \tag{3.9}$$

$$\Phi = \frac{1}{\sqrt{2N_f}}(\sigma + i\eta')I + (a_a + i\pi_a)T^a, \tag{3.10}$$

where we have introduced the matrix Φ, which is invariant under the unitary $U(N_f)\times U(N_f)$ transformations, and $\lambda_a,\ \lambda'_\sigma,\ \alpha$ and m are parameters of the model [7], [25].

The chiral symmetry is spontaneously broken via the σ field acquiring a VEV, i.e. $SU(N_f)_L \times SU(N_f)_R \times U(1)_V \to SU(N_f)_V \times U(1)_V$, as described in detail in section 2.2.

Meanwhile, the determinant term proportional to the parameter α breaks the axial symmetry $U(1)_A$. The corresponding VEV of the Φ matrix is then

$$\langle \Phi \rangle = \frac{v}{\sqrt{2N_f}}, \; f_\pi = \sqrt{\frac{2}{N_f}} v, \tag{3.11}$$

where f_π denotes the pion decay constant [7] and v is the temperature dependent QCD order parameter. More on broader theoretical aspects and recent developments of, specifically, two-flavour LσM can be found in Ref.[24].

One may also visualize how spontaneous chiral symmetry breaking is related to the σ meson. Considering the LσM potential in equation (3.9) for the two quark flavour case and only the lightest states in the theory, i.e. the σ and the π mesons, the potential may be plotted. This is best done in the polar coordinates, where σ would represent the radial coordinate, while π_a the rotation. As presented in Ref. [26] the resulting shape is the well-known "Mexican hat" potential. Without explicit chiral symmetry breaking terms, the obtained potential is symmetric around the rotational axis and has minima at a scale Λ_σ, where $\Lambda_\sigma^2 = \sigma^2 + \pi_a^2$. However, once the σ field acquires a VEV, the chiral symmetry is broken. This is due to the fact that the vacuum state must be invariant under parity. Implying that $\langle \sigma \rangle = \pm \Lambda_\sigma$. Then, the explicit chiral symmetry breaking terms are added in the Lagrangian by hand and would contain bare quark masses obtained from the Higgs field. The inclusion of these terms tilts the potential. Hence, creating a global minimum at either of $\pm \Lambda_\sigma$.

3.4 Implementing the combined model

We wish to investigate the DM particles arising from the confined dark Yang-Mills theory where all three of the aforementioned models are considered. In this section we present the main assumptions in our investigation used to combine these models, as well as introduce the interaction terms arising from the underlying fields. The relevant terms are $\mathcal{L}_{\text{gb+PL}}$ for interaction between the glueballs and the Polyakov loop, $\mathcal{L}_{\text{PL}\sigma\text{M}}$ the Polyakov loop extended LσM and $\mathcal{L}_{\text{gb + L}\sigma\text{M}}$ for interaction between the glueball and the LσM.

One of the main assumptions which we make is choosing to limit our investigation only to two quark flavours, the up- and the down-quarks, and to only the lightest states present in the model. Meaning, we neglect the presence of the scalar meson a and pseudoscalar meson η' from equation (3.10) in the LσM. On top of this, we choose to replace the exact Lagrangian of the LσM presented in equations (3.8) and (3.9) with a LσM-like Lagrangian as presented in Ref. [6]. This implies replacing the potential in equation (3.9) by a quartic Higgs-like potential. While simplifying the following analysis, this shape of the LσM Lagrangian still captures the essential physics for this study. In this form of the LσM the explicit chiral symmetry breaking terms are then added in form of lightest

scalar and pseudoscalar mesons. For the two quark flavour case these are the $\pi^{\pm}$ and π^0 mesons [6]. The resulting new Lagrangian of the LσM takes the shape of

$$\begin{aligned}\mathcal{L}_\sigma =&\frac{1}{2}\partial_\mu\sigma\partial^\mu\sigma + 2g^2v_0^2\sigma^2 + g^4\sigma^4 + \\ &\frac{1}{2}\partial_\mu\pi_\alpha\partial^\mu\pi_\alpha - \kappa g^2(m_u+m_d)\sigma^2\pi_\alpha\pi_\alpha,\end{aligned} \tag{3.12}$$

where m_u and m_d represent the up- and down-quark masses respectively, g is a coupling constant and κ is a constant defined in equation (2.9) .

Further, we chose to limit our investigation to the case of $N = 3$ colours and impose the reality condition on the expectation value of the Polyakov loop l, which reduces the Polyakov loop potential in equation (3.5) to

$$V(l) = T^4\left(-\frac{b_2(T)}{2}l^2 + b_4l^4 - 2b_3l^3\right). \tag{3.13}$$

We make this simplification based on the analysis conducted in section 3.2, where we noted that the difference between the gauge groups $N = 3, 4, 5$ is small. We leave the investigation to higher gauge groups for a potential future study.

The interaction between the Polyakov loop l and the glueball field ϕ is expressed through a term of the form [4]:

$$\begin{aligned}\mathcal{P}(l) =& c_1l^2, \\ \mathcal{L}_{\text{gb + Pl}} =& \frac{\phi^4}{2^8c^2}\mathcal{P}(l)\end{aligned} \tag{3.14}$$

where the form of $\mathcal{P}(l)$ is the lowest order satisfying the underlying gauge symmetries, and c_1 represents a free parameter. In Refs. [4] and [5] the value of the c_1 parameter for $SU(3)$ gauge group was found to be $c_1 = 1.225 \pm 0.19$ at 95 % confidence level. This value was obtained through investigating the behaviour of the glueball field VEV as a function of temperature.

The interaction between the glueball and the LσM, specifically for the two quark flavour ϕ-σ and ϕ-π_α interaction, enters through a term of the form [27]

$$\mathcal{L}_{\text{gb+L}\sigma\text{M}} = -m_0^2\,\text{Tr}\left[\left(\frac{\phi}{4c^{1/2}\Lambda e^{-1/4}}\right)^2\Phi^\dagger\Phi\right], \tag{3.15}$$

analogous to the term describing interaction between the chiral partners in the LσM in equation (3.9). Expanding the Φ matrix according to its definition in equation (3.10), and neglecting states heavier than σ and π_a, one obtains

$$\mathcal{L}_{\text{gb+L}\sigma\text{M}} = -\frac{m_0^2}{16\ c\ \Lambda^2\ e^{-1/2}}\phi^2(\sigma^2 + \pi_\alpha\pi_\alpha). \tag{3.16}$$

The nature of the parameter m_0 and its connection to chiral symmetry breaking has been heavily discussed in the literature [28, 29, 30, 31]. Particularly Ref. [28] considered a QCD-like model and expressed the dependence of the value of the parameter as a combination of σ meson mass, π mass and η mass alongside other parameters of the model. Since the particular combination present in our study has yet to be explored in the literature, we choose to treat m_0 as a free parameter of the theory.

The interaction between the Polyakov loop and the LσM is described via the so-called Polyakov loop extended LσM (PLσM) [7], [32]. The form of this term is similar to other interaction terms in the LσM, namely

$$\mathcal{L}_{\mathrm{PL}\sigma\mathrm{M}} = g_2 T^2 l^2 \,\mathrm{Tr}\left(\Phi^\dagger \Phi\right) = g_2 T^2 l^2 (\sigma^2 + \pi_\alpha \pi_\alpha), \tag{3.17}$$

where g_2 is a free, positive parameter [33].

For ease of working with the expressions, we redefine our parameters of the theory and associated constants in a more compact form. In further work, we make use of the following definitions:

$$\begin{aligned} &\lambda_{\sigma\pi} = \kappa g^2 (m_u + m_d),\ \lambda_\sigma = g^4,\ \lambda_{\sigma\phi} = -\frac{9\ e\ m_0^2}{2\ \Lambda^2}, \\ &\mu_\sigma^2 = -2 g^2 v_0^2,\ \nu = \frac{81}{2} e,\ \tau = \frac{\nu}{2} c_1 \end{aligned} \tag{3.18}$$

and introduce a re-scaled version of the confinement scale Λ as $\Lambda_1 = \Lambda 4\sqrt{c}$, with c defined in equation (3.1). As a result of the above assumptions and equations (3.12), (3.14), (3.13), (3.16) and (3.17) the total effective Lagrangian of our theory may be expressed as

$$\mathcal{L}_{\mathrm{tot}} = \frac{1}{2}\partial_\mu \phi \partial^\mu \phi + \frac{1}{2}\partial_\mu \sigma \partial^\mu \sigma + \frac{1}{2}\partial_\mu \pi_\alpha \partial^\mu \pi_\alpha - V_{\mathrm{tot}}(T, \phi, \sigma, l) \tag{3.19}$$

$$\begin{aligned} V_{\mathrm{tot}}(T, \phi, \sigma, l) = {} & \mu_\sigma^2 \sigma^2 + \lambda_\sigma \sigma^4 + \nu \phi^4 \log\left(\frac{\phi}{\Lambda_1}\right) + \\ & \lambda_{\sigma\pi} \sigma^2 \pi_\alpha \pi_\alpha + \lambda_{\sigma\phi} \phi^2 (\sigma^2 + \pi_\alpha \pi_\alpha) + \tau l^2 \phi^4 + \\ & g_2 T^2 l^2 (\sigma^2 + \pi_\alpha \pi_\alpha) + T^4 \left(-\frac{b_2(T)}{2} l^2 + b_4 l^4 - 2 b_3 l^3\right), \end{aligned} \tag{3.20}$$

with the form of $b_2(T)$ presented in equation (3.6). Further, we wish to exclude the explicit dependence on the Polyakov loop l from our Lagrangian. To this end, we calculate the stationary points of the Polyakov loop in the vacuum using the extrema condition

$$\frac{\partial V(T, \phi, \sigma, \pi_\alpha, l)}{\partial l} = 0, \tag{3.21}$$

which yields the solutions $l = 0$ and

$$l_\pm = \frac{3\ b_3\ T^2 \pm \sqrt{9\ b_3^2\ T^4\ +\ 4\ b_2(T)\ b_4\ T^4\ -\ 8\ g_2\ b_4\ T^2\ \sigma^2\ -\ 8\ \tau\ b_4\ \phi^4}}{4\ b_4\ T^2}. \tag{3.22}$$

Investigating the stability conditions, we identify that the solution l_+ represents the global minimum, $l = 0$ the local minimum, while the solution l_- is a maximum separating these two minima. This observation agrees with analogous calculation performed in Ref. [5] where the LσM was not considered. Hence, in further calculations, the explicit dependence on the Polyakov loop l is "integrated out" through the use of its equation of motion $l = l_+ = l(T, \phi, \sigma)$ and the potential is expressed as $V_{\rm tot}(T, \phi, \sigma, l(T, \phi, \sigma)) = V_{\rm tot}(T, \phi, \sigma)$.

4 COSMOLOGICAL EVOLUTION

In this section we introduce the theory and the basis of the methodology employed in investigating the thermal/time evolution of DM in an evolving Universe. To this end, we gain inspiration from the analysis carried out in Refs. [4] and [5] where the relic abundance of DM only in the form of glueballs was considered. We extend the formalism with the inclusion of the LσM in this section, and then present our findings in section 5.

During our analysis of the cosmological evolution of the glueball ϕ and σ fields we choose to treat them as classical background fields. Further, we are considering a dark sector, i.e., it does not interact with the SM. This allows us to approach the problem from a simplified perspective and make a direct comparison with the results presented in Ref. [4]. The obtained results could then be compared with the quantum treatment through the use of the generating functional method outlined in section 6. As a consequence of this assumption, we are required to remove all parts containing π dependence from equation (3.19) as pions do not form a classical condensate. Thus, for the purposes of investigating the cosmological evolution, the effective Lagrangian of the theory reduces to

$$\mathcal{L} = \frac{1}{2}\partial_\mu\phi\partial^\mu\phi + \frac{1}{2}\partial_\mu\sigma\partial^\mu\sigma - V(T, \phi, \sigma) \tag{4.1}$$

$$\begin{aligned} V(T, \phi, \sigma) =& \mu_{\sigma 2}\sigma^2 + \lambda_\sigma\sigma^4 + \lambda_{\sigma\phi}\phi^2\sigma^2 + \tau\phi^4 l^2 + \nu\phi^4 \log\left(\frac{\phi}{\Lambda_1}\right) + \\ & T^2 g_2 \sigma^2 l^2 + T^4\left(-\frac{b_2(T)}{2}l^2 + b_4 l^4 - 2b_3 l^3\right). \end{aligned} \tag{4.2}$$

As a first-order approximation, the glueball ϕ and the σ fields may be considered as homogeneous. As such, their evolution takes place in an expanding Friedmann-Lemaitre-Robertson-Walker (FLRW) Universe. For a general, homogeneous field ψ evolving in the FLRW Universe the Klein-Gordon equation may be written as

$$\ddot{\psi} + 3H\dot{\psi} + \partial_\psi V(T, \psi) = 0, \tag{4.3}$$

where H represents the Hubble parameter and dots represent the first and second derivatives with respect to cosmological time $H = 1/2t$ respectively. Denoting the photon temperature as T_γ, we may exchange cosmological time with photon temperature according to

their relation in the radiation-domination era:

$$t = \frac{1}{2}\sqrt{\frac{45}{4\pi^3 g_{*,\rho}(T_\gamma)}}\frac{m_P}{T_\gamma^2}, \tag{4.4}$$

with $g_{*,\rho}(T_\gamma)$ representing the number of interacting degrees of freedom of the SM bath at temperature T_γ and $m_P = 1.22 \cdot 10^{22}$ MeV is the Planck mass. Assuming that the dark sector in our investigation has no interactions with the visible SM sector, it is safe to impose that the number of interacting degrees of freedom in our theory is less that that of the SM. Consequently, the temperature of the dark sector is lower than the SM thermal bath. We define the ratio between these temperatures as ξ_T. This in turn allows us to relate the number of interacting degrees of freedom in the two sectors in terms of temperatures T_γ and T as $g_{*,\rho}(T_\gamma) = g_{*,\rho}(\xi_T T)$, with T being the temperature of the dark sector, entering in relations derived in the previous sections. Combining this with the temperature dependent cosmological time definition in equation (4.4) the Klein-Gordon equation (4.3) may be rewritten as

$$\frac{4\pi^3 g_{*,\rho}}{45 m_P^2}\xi_T^4 T^6 \frac{d^2\psi}{dT^2} + \frac{2\pi^3}{45 m_P^2}\frac{dg_{*,\rho}}{dT}\xi_T^4 T^6 \frac{d\psi}{dT} + \partial_\psi V(T,\psi) = 0. \tag{4.5}$$

When considering a wide range of temperatures, such as in the context of evolving Universe, the middle term may be neglected. We do this based on the fact that the number of interacting degrees of freedom remains approximately constant during the evolution of the Universe [4] [5]. This approximation is strongly violated during periods of large entropy production, such as, formation of the cosmological microwave background or period of early large scale structure formation. However, we choose to ignore the contributions arising from such events for the sake of retaining simplicity in our investigation. We suspect that if one where to keep the number of interacting degrees of freedom as a varying quantity, the difference in the obtained results would be small or even negligible. Treating $g_{*,\rho}$ as a constant enables us to reabsorb it in the definition of the visible-to-dark temperature ratio ξ_T as $\xi_T' = g_{*,\rho}\xi_T$.

The cosmological evolution of classical fields is analogous to that of a dampened oscillator in a non-linear potential around its minimum. This analogy allows us to define the energy-density ρ of the evolving field ψ as

$$\rho = \frac{2\pi^3}{45 m_P^3}\xi_T'^4 \left(\frac{d\psi}{dT}\right)^2 + V(T,\psi). \tag{4.6}$$

As described in Refs. [34] and [4] as long as harmonic oscillator approximation remains valid the energy-density should behave as $\sim T^3$, in the case of cold dark matter (CDM).

A straightforward extension of equations (4.5) and (4.6) in the case of two evolving fields

gives

$$\frac{4\pi^3 g_{*,\rho}}{45m_P^2}\xi_T^4 T^6 \frac{d^2\phi}{dT^2} + \partial_\phi V(T,\phi,\sigma) = 0, \tag{4.7}$$

$$\frac{4\pi^3 g_{*,\rho}}{45m_P^2}\xi_T^4 T^6 \frac{d^2\sigma}{dT^2} + \partial_\sigma V(T,\phi,\sigma) = 0, \tag{4.8}$$

$$\rho = \frac{2\pi^3}{45m_P^3}\xi_T'^4 \left[\left(\frac{d\phi}{dT}\right)^2 + \left(\frac{d\sigma}{dT}\right)^2\right] + V(T,\phi,\sigma), \tag{4.9}$$

where now we have two Klein-Gordon equations - equation (4.7) for the glueball field ϕ and equation (4.8) for the σ-field. While the potential $V(T,\phi,\sigma)$ is given by equation (4.2). Further, we introduce a dimensionless constant μ as

$$\mu^2 = \frac{4\pi^3 \xi_T'^4 \Lambda^2}{45m_P^2}, \tag{4.10}$$

where Λ is the confinement scale discussed in section 3, not to be confused with our re-scaled version Λ_1. Following Ref. [4] we rewrite the obtained relations in terms of dimensionless variables through the use of redefinitions:

$$\phi = \Lambda\ \tilde{\phi},\ \sigma = \Lambda\ \tilde{\sigma},\ V = \Lambda^4\ \tilde{V},\ T = \Lambda\ \tilde{T} \tag{4.11}$$

Hence, the equations (4.7) - (4.9) take the following form:

$$\mu^2 \tilde{T}^6 \frac{d^2\tilde{\phi}}{d\tilde{T}^2} + \partial_{\tilde{\phi}}\tilde{V}(\tilde{T},\tilde{\phi},\tilde{\sigma}) = 0, \tag{4.12}$$

$$\mu^2 \tilde{T}^6 \frac{d^2\tilde{\sigma}}{d\tilde{T}^2} + \partial_{\tilde{\sigma}}\tilde{V}(\tilde{T},\tilde{\phi},\tilde{\sigma}) = 0, \tag{4.13}$$

$$\tilde{\rho} = \frac{\mu^2\tilde{T}^6}{2}\left[\left(\frac{d\tilde{\phi}}{d\tilde{T}}\right)^2 + \left(\frac{d\tilde{\sigma}}{d\tilde{T}}\right)^2\right] + \tilde{V}(\tilde{T},\tilde{\phi},\tilde{\sigma}), \tag{4.14}$$

which we make use of in the numerical analysis in the next section.

5 NUMERICAL RESULTS

We present the numerical results obtained for cosmological evolution of the glueball ϕ and the σ-fields coupled to the Polyakov loop l. We first present the results obtained for the case where both fields, coupled to the Polyakov loop, are treated separately. Then present the combined case described by the Lagrangian in equation (4.1). We make comparisons to the results presented in Ref. [4] where applicable.

In section 3.4 in our description of the theory we have introduced many free parameters. After making use of the redefinition in equation (3.18), we are left with 8 free parameters: $\lambda_\sigma,\ \lambda_{\sigma\phi},\ \mu_\sigma^2, c_1, g_2, \nu$ as well as the confinement scale Λ and μ entering through equations (4.12) - (4.14). As the confinement scale Λ enters also in the aforementioned equations, we present its values rather than those of the rescaled version Λ_1. Additionally, since we wish for the value of the VEV of the Polyakov loop l to remain positive throughout our investigation, we may make use of this to reduce the number of free variables. Firstly, we fix the values of $c_1 = 1.225$ as per Ref. [4]. Secondly, we set $g_1 = 1.0$ since the only mention of its numerical value in the literature is that its a positive parameter [33]. We note that the values of these parameters may be adjusted in future investigations, as they would have impact on the total relic density of DM today as well as the masses of the σ meson and the glueball.

To determine physically appropriate values of the remaining free parameters we calculate the Hessian matrix in the vacuum, which is a matrix containing the second derivatives of the potential in equation (4.2) with respect to the fields. This is done in combination with arbitrary values of the ϕ and the σ field VEVs. This enables us to pick those values of the parameters which relate to physically allowed, i.e. positive, masses for the glueball and the σ meson in vacuum. The equations for the masses in terms of parameters of the theory read:

$$\begin{aligned} m_\phi^2 = &-2\Big(-2\phi^2\nu + \sigma^2(-2\lambda_\sigma + \lambda_{\phi\sigma}) + \\ &\sqrt{4\phi^4\nu^2 + \sigma^4(2\lambda_\sigma + \lambda_{\phi\sigma})^2 + 4\sigma^2\phi^2(\lambda_{\phi\sigma}^2 - \nu(2\lambda_\sigma + \lambda_{\phi\sigma}))}\Big), \\ m_\sigma^2 = &\ 2\Big(2\phi^2\nu + \sigma^2(2\lambda_\sigma - \lambda_{\phi\sigma}) + \\ &\sqrt{4\phi^4\nu^2 + \sigma^4(2\lambda_\sigma + \lambda_{\phi\sigma})^2 + 4\sigma^2\phi^2(\lambda_{\phi\sigma}^2 - \nu(2\lambda_\sigma + \lambda_{\phi\sigma}))}\Big), \end{aligned} \tag{5.1}$$

where ϕ and σ are placeholders for their respective VEVs. Our scan was performed by letting the remaining 6 free variables take values in the range from -25 to 100. Throughout our scan for appropriate parameter values, we noted that in all physically allowed cases the mass of the σ meson m_σ was larger than that of the glueball m_ϕ. This opens the possibility that during some stage of the evolution the σ meson may decay into glueballs. This result is in contradiction with the current phenomenological predictions, where the σ meson has a mass of $m_\sigma \approx 520$ eV and the glueball $m_\phi \approx 1.71$ GeV. On top of this, independently of

the meson mass, there exists a possibility of a cannibalistic phase. During such a phase, the number of particles in the condensate reduces due to self-interactions, as described in detail for the glueball evolution in Ref. [4]. We leave the exploration of these features for a model containing both glueball and σ meson for a potential future study, and further will assume that both the σ meson and the glueball remain stable throughout their evolution.

We first present the form of the glueball and the LσM parts of the potential in equation (4.2) coupled with the Polyakov loop as a function of the field values in both the confined $T < T_c$ phase and the deconfined $T > T_c$ phase in Figures 4*a* and 4*b* respectively. Here and further T_c denotes the confinement-deconfinement phase transition critical temperature, given in terms of confinement scale Λ in equation (3.7). In the case of the glueball potential coupled to the Polyakov loop potential there is a clear distinction in the overall form of the potential and the location of the minimum of the potential between the two phases. These results match exactly with those presented in Ref. [4]. On the other hand, the behaviour of the LσM potential coupled to the Polyakov loop is more subtle. While the location of the minimum slightly shifts, the shape of the potential remains approximately the same. Hence, we expect the thermal evolution of the two fields to be noticeably different.

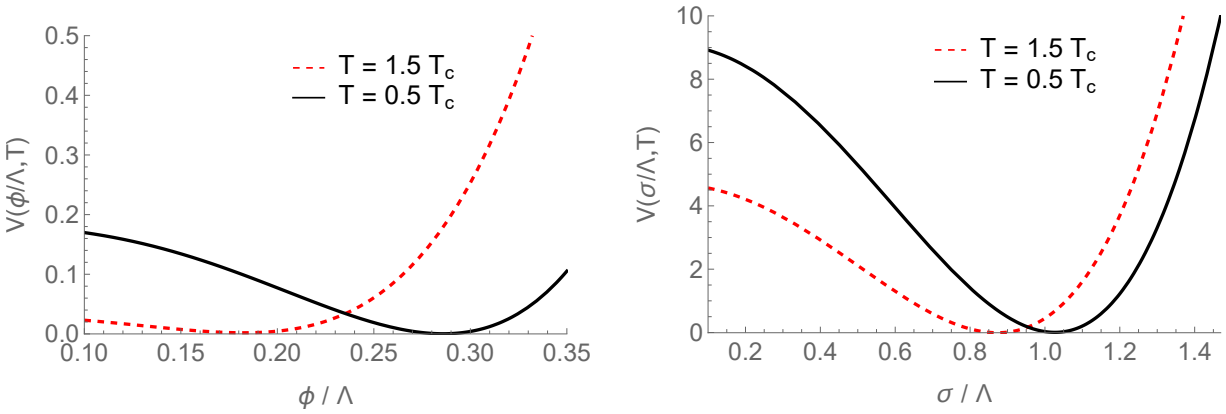

(a) (b)

Figure 4: Evolution of the (a) glueball and (b) LσM part of the potential in equation (4.2) coupled with the Polyakov loop l, as a function of values of the fields divided by the confinement scale Λ. The dashed line corresponds to the deconfined phase with $T = 1.5\ T_c$, and the solid line to confined phase with $T = 0.5\ T_c$. The minimum of the potential is set to correspond to zero.

Throughout the remainder of this section, the cases we chose to present where picked arbitrary as long as two conditions where satisfied. Firstly, the parameters represented physically viable glueball and σ meson masses, as per discussion above. Secondly, at the end of the evolution, the fields reside in their global minimum. The second condition was important to identify, as for certain choices of parameter values the field may never reach its global minimum during the evolution. Lastly, we remind the reader that the evolution in time takes place from high temperature to low temperature as the Universe is cooling

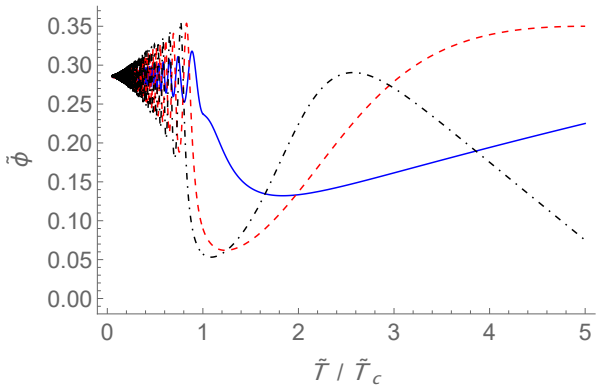

Figure 5: Thermal evolution of the glueball field $\tilde{\phi}$ as per Klein-Gordon equation (4.12) with parameter values $c_1 = 1.225$, $\Lambda = 1$, $\mu = 0.05$ for different, arbitrary initial conditions.

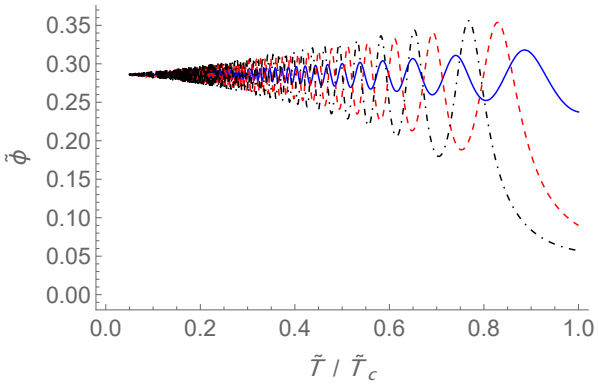

Figure 6: Evolution after the critical temperature T_c of the scenario displayed in Figure 5.

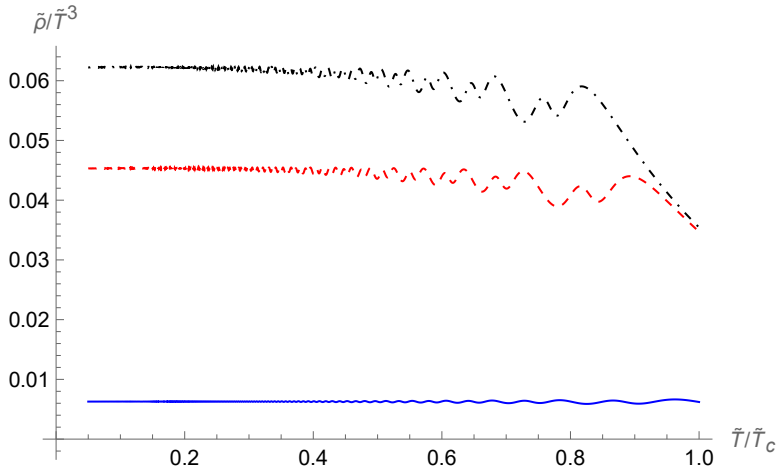

Figure 7: Thermal evolution of the energy-density $\tilde{\rho}$ in the case of glueball field ϕ coupled to the Polyakov loop l with parameter values $c_1 = 1.225$, $\Lambda = 1$, $\mu = 0.05$ according to equation (4.14) for the same initial conditions as in Figure 5.

down. The relation between cosmological time t and temperature of our dark sector T is presented in equation (4.4).

The thermal evolution of the glueball field ϕ for different, arbitrary initial conditions per equation (4.12) can be seen in Figure 5. In agreement with the results presented in Ref. [4] we find that different initial conditions, but the same choice of parameters c_1, Λ and μ, do not have an impact on the VEV of the ϕ field in the confined phase. It is rather the parameter values which alter the location of the minimum in the potential. Initial conditions do however impact the evolution in the deconfined phase and the amplitude

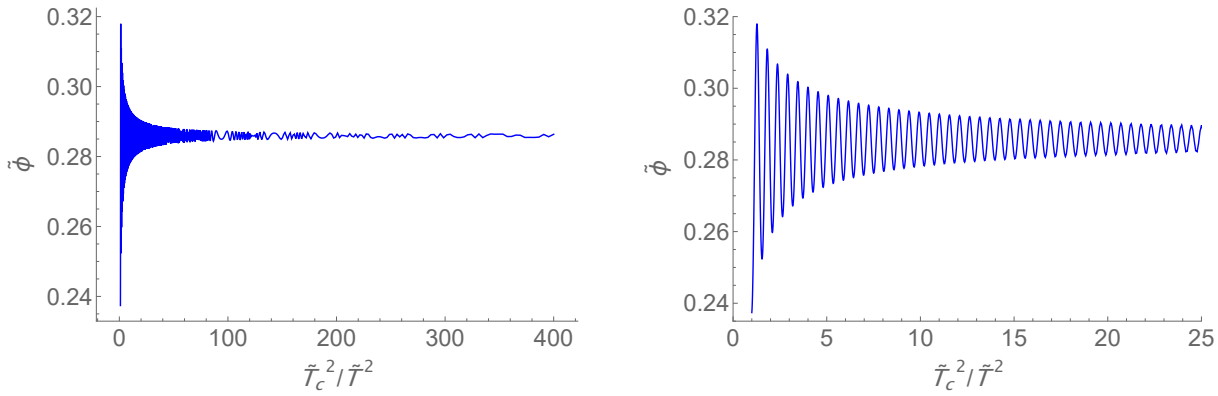

(a) (b)

Figure 8: Evolution in cosmological time ($t \propto 1/T^2$) in the confined phase of the glueball field ϕ with parameter values $c_1 = 1.225, \Lambda = 1,\ \mu = 0.05$. The displayed case is for the same initial conditions as the blue line in Figure 5. The zero point denotes the point of the confinement-deconfinement phase transition. (a) displays evolution down to $\tilde{T} = 0.05$, and (b) a zoomed in look at the periodic oscillations right after confinement.

of oscillations around the VEV of the field. Notably, there are two different evolutionary paths for the glueball field ϕ in the deconfined phase, which can be seen by comparing the blue and red lines in Figure 5. Further, as can be seen in Figures 6 and 7, larger amplitude of oscillations around the ϕ VEV imply larger final energy density ρ of the DM. We also present a single example of evolution in time in the confined phase in Figure 8. To this end, we make use of the relation $t \propto 1/T^2$ in equation (4.4). We find that right after the confinement-deconfinement phase transition there are periodic oscillations with a large amplitude, which dampen as the Universe keeps cooling down. Additionally, after a certain point, the oscillations become non-periodic. If the calculation where to be carried out to $T \longrightarrow 0$ the oscillations of the field around its VEV would halt completely. The observed behaviour is similar for all of the displayed cases.

Similar analysis holds true for the thermal evolution of the σ field in Figure 9 and the associated energy density in Figure 11. The difference is that the thermal evolution of the σ field is less sensitive to the initial conditions. Independently of the initial conditions, the σ field follows a characteristically similar evolution for any choice of initial conditions in both the confined and the deconfined phase. On top of this, the amplitude of oscillations in the confined phase is also less sensitive to the initial conditions in the confined phase, as can be seen by comparing Figures 6 and 10.

Comparing Figures 5 and 9 we note that the behaviour of the two fields in the deconfined phase is very different. While the glueball field tends to evolve to a value lower than its VEV before the critical temperature, the σ field initiates oscillations with a large amplitude, which dampen as the Universe cools down. On the contrary, the behaviour in the confined phase for both fields is very similar, where both fields oscillate around their VEVs. This

can be seen in Figures 6 and 10.

We also note that the impact of the confinement-deconfinement phase transition is more noticeable in the evolution of the glueball field ϕ than in the evolution of the σ field. Particularly, the glueball field experiences a large increase in its value at the critical temperature, followed by oscillations around its VEV. Meanwhile the impact of the phase transition on the evolution of the σ field is smaller. The only notable consequence of the phase transition is that the oscillations dampen faster. A possible reason for the displayed behaviour of the σ field could be our simplification of treating the fields as classical and removing the quark contributions of the LσM. Hence, not capturing explicit chiral symmetry breaking.

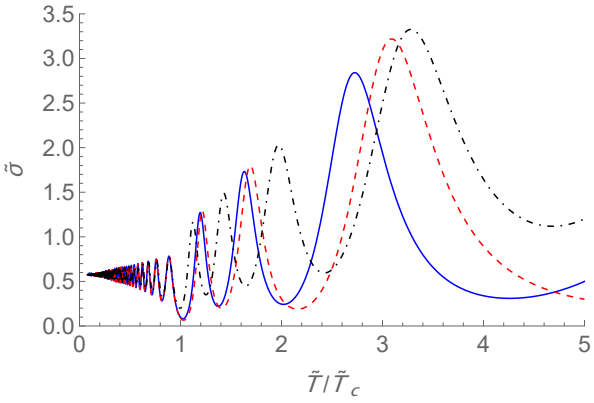

Figure 9: Thermal evolution of the $\tilde{\sigma}$ field as per Klein-Gordon equation (4.13) with parameter values $\mu_\sigma^2 = -17.237$, $\lambda_\sigma = 8.177,\ \lambda_{\sigma\phi} = 0.635,\ \nu = 18.869,$ $\Lambda = 1.781,\ \mu = 0.005,\ g_2 = 1.0$ for different initial conditions.

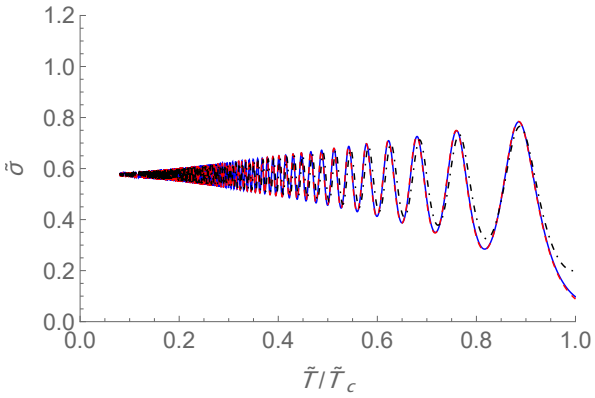

Figure 10: Evolution after the critical temperature T_c of the scenario displayed in Figure 9.

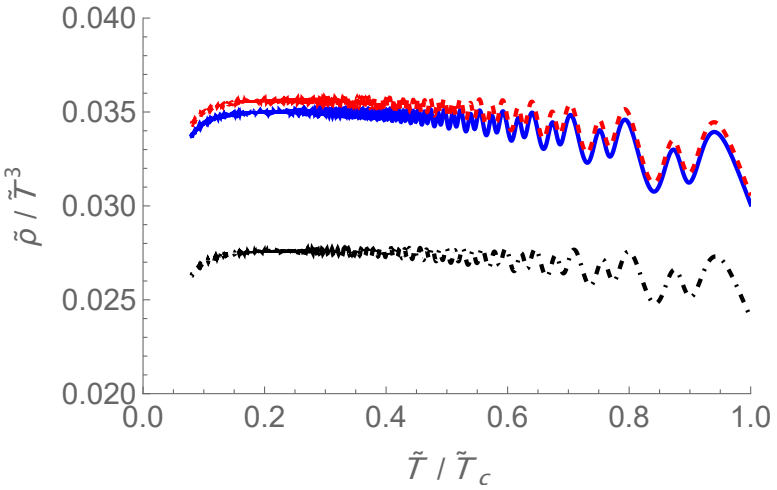

Figure 11: Thermal evolution of the energy-density $\tilde{\rho}$ in the case of σ field coupled to the Polyakov loop l with parameter values $\mu_\sigma^2 = -17.237,\ \lambda_\sigma = 8.177,\ \lambda_{\sigma\phi} = 0.635,$ $\nu = 18.869,\ \Lambda = 1.781,\ \mu = 0.005,\ g_2 = 1.0$ for the same initial conditions as in Figure 9.

The cosmological evolution of the simplified model described by the Lagrangian in equation (4.1) is presented in Figures 12, 13 and 14. We have investigated two scenarios, in Figure 12 the glueball and the σ meson masses are comparable, while in Figure 13 the mass of the σ is more than two times larger than that of the glueball. We do not find any notable differences in the evolution of the fields or energy densities between the two cases. Therefore, we present the evolution of energy-density in the large mass difference case in Figure 14.

The obtained results differ from those discussed above. Firstly, the behaviour before and at the critical temperature has slightly changed. The glueball field no longer drops in value below its VEV before the phase transition and rather exhibits an oscillatory behaviour around its VEV. We hypothesize that this is due to the coupling between the fields, as this behaviour is more characteristic of the σ field evolution. Secondly, the oscillations of the σ field in the deconfined phase are not present. This in turn, is more characteristic of the glueball field ϕ. Thirdly, the values of the VEVs of the fields have changed. We note that the values of the σ field VEV slightly differs between the two displayed cases. However, this is only due to the displayed parameter choices. On the other hand, the VEV of the glueball field ϕ remained approximately the same through out our parameter scan. This implies that the evolution of the σ field is more sensitive to the choice of the parameters.

Comparing the evolution of the energy density for the combined model in Figure 14 with those where the fields are treated independently in Figures 7 and 11, we make the following observation. Right after the phase transition the evolution is still impacted due to changes in dynamics of mostly the glueball field, while the amplitude of the oscillations is suppressed from contributions of the σ field.

Lastly, we would like to make a remark regarding the displayed energy-density results. The "tails" noticeable in the evolution of the energy density in Figures 7, 11 and 14 arise due to numerical rounding errors and do not have any impact on the displayed physics. According to methods presented in Ref. [4] the resulting relic density of the DM today may be calculated by using $\tilde{T}_f/\tilde{T}_c = 0.1$. This cutoff would imply completely ignoring the effects of these "tails" on the resulting relic density of DM today.

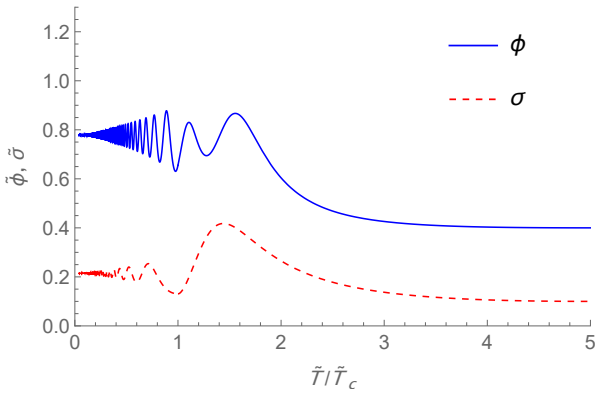

Figure 12: Thermal evolution of the glueball ϕ combined with the LσM where both are coupled to the Polyakov loop l as per Klein-Gordon equations (4.12) and (4.13) with parameter values of $\mu_\sigma^2 = -33.338$, $\lambda_\sigma = 13.015$, $\lambda_{\sigma\phi} = -0.099$, $\nu = 16.077$, $g_2 = 1.0$, $c_1 = 1.225$, $\Lambda = 5.416$, $\mu = 0.0004$ for arbitrary initial conditions. In the displayed case the masses of the glueball and σ meson are comparable. The dashed line displays the evolution of the σ field, and the solid line the evolution of the glueball field ϕ.

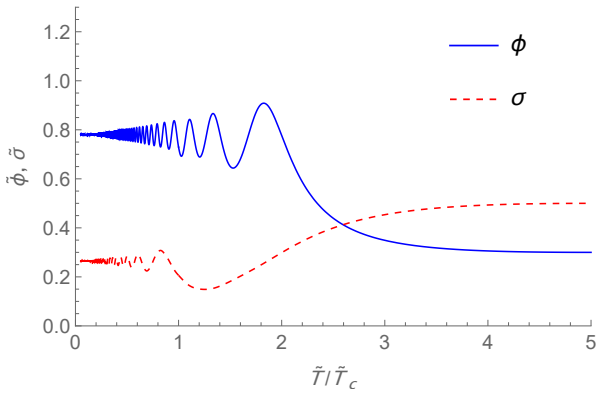

Figure 13: Thermal evolution of the glueball ϕ combined with the LσM where both are coupled to the Polyakov loop l as per Klein-Gordon equations (4.12) and (4.13) with parameter values of $\mu_\sigma^2 = -0.4372$, $\lambda_\sigma = 26.049$, $\lambda_{\sigma\phi} = -5.787$, $\nu = 72.635$, $g_2 = 1.0$, $c_1 = 1.225$, $\Lambda = 1.937$, $\mu = 0.001$ for arbitrary initial conditions. In the displayed case the mass of the σ meson is much larger than that of the glueball. The dashed line displays the evolution of the σ field, and the solid line the evolution of the glueball field ϕ.

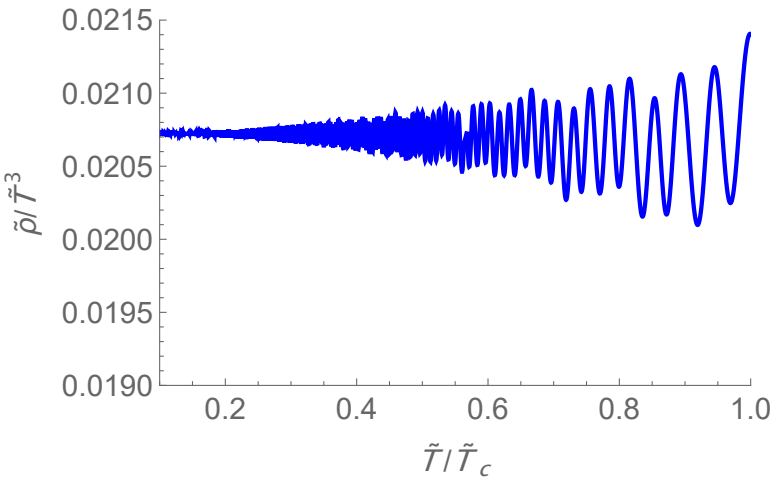

Figure 14: Thermal evolution of the energy-density for glueball field ϕ combined with the LσM where both are coupled to the Polyakov loop l according to equation (4.14) with parameter values of $\mu_\sigma^2 = -0.4372,\ \lambda_\sigma = 26.049,\ \lambda_{\sigma\phi} = -5.787,\ \nu = 72.635, g_2 = 1.0,$ $c_1 = 1.225,\ \Lambda = 1.937,\ \mu = 0.001$ for the scenario displayed in Figure 13.

Using the results displayed in Figure 14 one may calculate the phase transition scale Λ_0 at which the σ mesons and the glueballs become the totality of DM. This may be carried out using the relations presented in Ref. [4]. Namely, first one averages the last oscillations in energy-density:

$$\left\langle \frac{\tilde{\rho}}{\tilde{T}^3} \right\rangle = \frac{1}{0.3\tilde{T}_f} \int_{\tilde{T}_f}^{1.3\tilde{T}_f} \frac{\tilde{\rho}(\tau)}{\tau^3} d\tau. \tag{5.2}$$

Ref. [4] mentions that this quantity saturates to a value independent of the phase transition scale Λ. However, it does retain dependence on the choice of other parameters of the theory. The relic density of DM today may then be calculated by accounting for the expansion of the Universe:

$$\Omega_{\rm DM} h^2 = \frac{\Lambda}{\rho_c/h^2} \left\langle \frac{\tilde{\rho}}{\tilde{T}^3} \right\rangle T_f^3 \left(\frac{T_{\gamma,0}}{\xi_T T_f} \right)^3 = 0.12 \xi_T^{-3} \frac{\Lambda}{\Lambda_0}, \tag{5.3}$$

where $\rho_c/h^2 = 1.05 \cdot 10^4$ eV cm^{-3} is the critical density, $h = 0.674$, ξ_T the ratio in temperature between the visible and the dark sectors, and $T_{\gamma,0} = 0.235$ meV is the temperature of the visible photon bath today. Carrying out this calculating for the case presented in Figure 14 we find that $\Lambda_0 \approx 3.24$ eV. Which is two orders of magnitude lower than the results presented in Ref. [4] and would imply that our DM freezes out too late in the evolution of the Universe. To obtain results which better agree with the previous studies, we would require more data from the lattice simulations. This would allow us to fix more

of our free parameters and perform a scan over the remainder of the free parameters, focusing on the regions which would yield $\Lambda_0 \sim 130$ eV. Once such values are obtained and suitable range of values for the remaining free parameters are identified, a scan over the temperature ratio between the dark and visible sectors ξ_T may also be performed. Such result for only the glueball coupled to the Polyakov loop was displayed in Ref. [4]. The importance of this result is that it allows one to identify the epoch of cosmological evolution at which the freeze-out of DM takes place, and imposes further constraints on the dark sector considered.

6 GENERATING FUNCTIONAL

The LσM by definition describes the quark condensate for the zero temperature case. However, as it is well established, the evolution of the Universe is accompanied by a gradual decrease in temperature. Over cosmological timescales the temperature changes by several orders of magnitude. Consequently, the thermodynamic variables describing the condensate change as well. In this section, we follow closely the methods presented in Ref. [6]. It introduces the generating functional method as a means of investigating thermal evolution of thermodynamic observables describing a condensate containing quantum fields in cosmology. We apply the generating functional formalism to our extended model, however, due to time constraints and hurdles during the project have not been able to finish the calculations. Therefore, we present the obtained derivations and references to the necessary further steps, leaving the completion of the investigation as a potential starting point of a future study.

The main motivation for choosing the generating functional method is that it by construction accounts for quantum fluctuations. Hence, incorporating further temperature dependence in our model outside of the Polyakov loop. To this end, one considers oscillations of the fields about their VEVs as quanta. The necessary derivations are more straightforward than in alternate methods, such as, the Cornwall-Jackiw-Tomboulist (CJT) method used in Ref. [7].

To further reduce the complexity we assume that the glueball field ϕ may be treated as a spatially constant background field. This is done on the phenomenological basis that the most probable glueball state is a lot heavier than that of σ, $\pi^{\pm}$ and π^0 mesons. While this contradicts with the observation made in section 5, we believe that addition of explicit chiral symmetry breaking terms and accounting for thermal effects would lead to more phenomenologically consistent results. Considering the glueball field to be a background field implies dropping the associated kinetic term in the effective Lagrangian describing our theory in equation (3.19). Further, the glueball field is assumed to always be in its minimum, i.e., there will be no perturbation associated with taking its VEV. Then we

introduce the VEV of the σ-field as per [6]:

$$\sigma = \langle\sigma\rangle + \tilde{\sigma},\ \langle\sigma\rangle = \frac{v}{g}, \tag{6.1}$$

and use the approximations outlined in [35] and [36]. The approximations are based on resummation of daisy and superdaisy diagrams, which are higher order thermal corrections to the effective potential, and take the VEVs of σ and π_α fields to be independent, in this way incorporating the thermal corrections into the method. The implication of the approximation is that the VEVs of the fields are equal to zero for odd-point correlation functions and equivalent to functions of smaller order for even-point correlation functions. For our purposes this implies the following relations

$$\begin{aligned} &\langle\tilde{\sigma}^3\rangle = \langle\pi_\alpha\pi_\beta\tilde{\sigma}\rangle = \langle\pi_\alpha\tilde{\sigma}\rangle = 0, \\ &\langle\tilde{\sigma}^4\rangle = 3\langle\tilde{\sigma}^2\rangle, \\ &\langle\pi_\alpha\pi_\alpha\tilde{\sigma}^2\rangle = \langle\pi_\alpha\pi_\alpha\rangle\langle\tilde{\sigma}^2\rangle. \end{aligned} \tag{6.2}$$

The equation of state $v(T)$ of the condensate is then obtained through the usage of the above approximations and the equations of motion:

$$v(T)^2 = \frac{2g^2v_0^2 - \lambda_{\sigma\pi}\langle\pi_\alpha\pi_\alpha\rangle - 6g^4\langle\tilde{\sigma}^2\rangle - \lambda_{\sigma\phi}\ \phi^2 - g_2T^2l^2}{2g^2}, \tag{6.3}$$

with the Polyakov loop $l = l(T, \phi, \sigma)$ expressed in its minima according to equation (3.22), and v_0 being the zero temperature QCD order parameter. According to methods presented in Ref. [6] we calculate the value of v_0 for the two quark flavour case to be $v_0 \approx 260\pm15$ MeV.

Then inserting the tadpole solution in the calculation of the Hessian matrix in the vacuum one may express the equations of motion of the σ and π_α mesons along side their temperature dependent masses as:

$$\partial_\mu\partial^\mu\tilde{\sigma} + m_\sigma^2\tilde{\sigma} = 0,\ m_\sigma^2 = 8g^2v^2, \tag{6.4}$$

$$\partial_\mu\partial^\mu\pi_\alpha + m_\pi^2\pi_\alpha = 0,\ m_\pi^2 = 2\kappa(m_u + m_d)\mathcal{M}^2, \tag{6.5}$$

where we have introduced

$$\mathcal{M}^2 \equiv v^2 + g^2\langle\tilde{\sigma}^2\rangle. \tag{6.6}$$

To establish a relationship between the effective Lagrangian and thermodynamic observables of the condensate we begin by defining the energy momentum tensor through its usual definition

$$\mathcal{T}_\nu^\mu \equiv \frac{\partial\mathcal{L}}{\partial(\partial_\mu\psi_\alpha)}\partial_\nu\psi_\alpha - \delta_\nu^\mu\mathcal{L}, \tag{6.7}$$

with ψ_α representing a general field, in our case σ and π_α. Applying this definition to the Lagrangian in equation (3.19) one obtains

$$\mathcal{T}^\mu_\nu = \partial_\nu\sigma\partial^\mu\sigma + \partial_\nu\pi_\alpha\partial^\mu\pi_\alpha - \delta^\mu_\nu\left(\mathcal{L}_{\text{tot}}\right). \tag{6.8}$$

Then, the free energy density, also commonly known as the generating functional, of the meson plasma is obtained via taking the VEV of the spatial trace of the energy-momentum tensor [6]

$$\mathcal{F} = \frac{1}{3}\langle\mathcal{T}^i_i\rangle. \tag{6.9}$$

Employing the relations given in equations (6.1), (6.2) and expanding the parameters μ_σ^2 and λ_σ according to their definitions in equation (3.18) one may express the generating functional as

$$\begin{aligned}\mathcal{F} = &-\frac{1}{3}\left(\langle\nabla\tilde{\sigma}\nabla\tilde{\sigma}\rangle + \langle\nabla\pi_\alpha\nabla\pi_\alpha\rangle\right) - \Bigg[\frac{1}{2}\langle\partial_\beta\tilde{\sigma}\partial^\beta\tilde{\sigma}\rangle + \frac{1}{2}\langle\partial_\beta\pi_\alpha\partial^\beta\pi_\alpha\rangle + 2v_0^2(v^2 + g^2\langle\tilde{\sigma}^2\rangle) - \\ &\lambda_{\sigma\pi}\left(\frac{v^2}{g^2} + \langle\tilde{\sigma}^2\rangle\right)\langle\pi_\alpha\pi_\alpha\rangle - \left(v^4 + 6g^2v^2\langle\tilde{\sigma}^2\rangle + 3g^4\langle\tilde{\sigma}^2\rangle^2\right) - \\ &\lambda_{\sigma\phi}\phi^2\left(\left(\frac{v^2}{g^2} + \langle\tilde{\sigma}^2\rangle\right) + \langle\pi_\alpha\pi_\alpha\rangle\right) - \tau l^2\phi^4 - \nu\phi^4\log\left(\frac{\phi}{\Lambda_1}\right) - \\ &T^2g_2l^2\left(\left(\frac{v^2}{g^2} + \langle\tilde{\sigma}^2\rangle\right) + \langle\pi_\alpha\pi_\alpha\rangle\right) - T^4\left(\frac{b_2(T)}{2}l^2 + b_4l^4 - 2b_3l^3\right)\Bigg]\end{aligned} \tag{6.10}$$

Using the self-consistency relation $\langle\partial_\mu\psi\partial^\mu\psi\rangle = m_\psi^2\langle\psi^2\rangle$ and making use of equation (6.6) we can simplify further to obtain

$$\begin{aligned}\mathcal{F} = &-\frac{1}{3}\left(\langle\nabla\tilde{\sigma}\nabla\tilde{\sigma}\rangle + \langle\nabla\pi_\alpha\nabla\pi_\alpha\rangle\right) + \\ &v^4 - \frac{m_\sigma^2}{2g^2}(\mathcal{M}^2 - v^2) + 6v^2(\mathcal{M}^2 - v^2) + 3(\mathcal{M}^2 - v^2)^2 - 2\mathcal{M}^2v_0^2 + \\ &\frac{\lambda_{\sigma\phi}}{g^2}\phi^2\mathcal{M}^2 + \frac{g_2T^2l^2}{g^2}\mathcal{M}^2 + (\lambda_{\sigma\phi}\phi^2 + g_2T^2l^2)\langle\pi_\alpha\pi_\alpha\rangle + \\ &\left(\nu\log\left(\frac{\phi}{\Lambda_1}\right) + \tau l^2\right)\phi^4 - T^4\left(\frac{1}{2}b_2l^2 + 2b_3l^3 - b_4l^4\right).\end{aligned} \tag{6.11}$$

As indicated in [6] the computation of VEVs of $\langle\nabla\tilde{\sigma}\nabla\tilde{\sigma}\rangle$ and $\langle\nabla\pi_\alpha\nabla\pi_\alpha\rangle$ produces temperature dependent relations of the form

$$\langle\nabla\phi\nabla\phi\rangle = J_2(T, m_\phi) + \frac{1}{2}\sum_{\vec{p}}\frac{p^2}{\omega_{p(\phi)}}, \tag{6.12}$$

where

$$
\begin{aligned}
J_n(T, m_\phi) &= \frac{1}{2\pi^2} \int_0^\infty \frac{p^{2n}}{\omega_{p(\phi)}} \frac{1}{e^{p(\phi)/T} - 1} \\
J_{n(\text{vac})}(m_\phi) &= \frac{1}{2} \sum_{\vec{p}} \frac{p^{2(n-1)}}{\omega_{p(\phi)}} \\
\omega_{p(\phi)} &= \sqrt{p^2 + m_\phi^2}
\end{aligned}
\tag{6.13}
$$

and p denotes the momentum of the mesons in the condensate, while $J_{n(\text{vac})}$ accounts for contributions arising from vacuum oscillations. For $n = 0, 1, 2$ these simplify as

$$
\begin{aligned}
J_{0(\text{vac})} &= -\frac{1}{8\pi^2} \ln \left[\frac{e\ m_\phi^2}{m_{\phi(\text{vac})}^2} \right], \\
J_{1(\text{vac})} &= \frac{1}{16\pi^2} \ln \left[\frac{m_\phi^2}{m_{\phi(\text{vac})}^2} \right], \\
J_{2(\text{vac})} &= -\frac{3}{64\pi^2} \ln \left[\frac{m_\phi^2}{\sqrt{e} m_{\phi(\text{vac})}^2} \right],
\end{aligned}
\tag{6.14}
$$

where $m_{\phi(\text{vac})}^2$ represents the mass of the meson in vacuum at zero temperature, and e the Euler's Number. We also take note of the derivatives of $J_n(T, m_\phi)$ with respect to m_ϕ and T, which will be useful in what follows,

$$
\begin{aligned}
\frac{\partial J_n(T, m_\phi)}{\partial m_\phi}\Big|_T &= -(2n-1) m_\phi J_{n-1}(T, m_\phi), \\
\frac{\partial J_n(T, T)}{\partial T}\Big|_{m_\phi} &= \frac{(2n-1)}{T} m_\phi^2 J_{n-1}(T, m_\phi) + \frac{2n}{T} J_n(T, m_\phi).
\end{aligned}
\tag{6.15}
$$

Now we may rewrite the expression for the generating functional in equation (6.9) purely in terms of variables of state $(T, v, m_\sigma, \mathcal{M})$ and the glueball field ϕ. We remind that the Polyakov loop is expressed at its minimum $l = l_+ = l(T, \phi, \sigma)$ according to equation (3.22):

$$
\begin{aligned}
\mathcal{F}(T, v, m_\sigma, \mathcal{M}) = &-\frac{1}{3} \left(J_2(T, m_\sigma) + 3 J_2(T, m_\pi) \right) + \\
&v^4 - \frac{m_\sigma^2}{2g^2} (\mathcal{M}^2 - v^2) + 6v^2 (\mathcal{M}^2 - v^2) + 3(\mathcal{M}^2 - v^2)^2 - 2\mathcal{M}^2 v_0^2 + \\
&\frac{\lambda_{\sigma\phi}}{g^2} \phi^2 \mathcal{M}^2 + \frac{g_2 T^2 l^2}{g^2} \mathcal{M}^2 + (\lambda_{\sigma\phi} \phi^2 + g_2 T^2 l^2) \langle \pi_\alpha \pi_\alpha \rangle + \\
&\left(\nu \log \left(\frac{\phi}{\Lambda_1} \right) + \tau l^2 \right) \phi^4 - T^4 \left(\frac{1}{2} b_2 l^2 + 2 b_3 l^3 - b_4 l^4 \right) + \\
&\frac{m_\sigma^4}{64\pi^2} \ln \left[\frac{m_\sigma^2}{\sqrt{e}\ m_{\sigma(\text{vac})}^2} \right] + \frac{3 m_\pi^4}{64\pi^2} \ln \left[\frac{m_\pi^2}{\sqrt{e}\ m_{\pi(\text{vac})}^2} \right]
\end{aligned}
\tag{6.16}
$$

where the factor of 3 in front of $J_2(T, m_\pi)$ originates from 3 pion species - $\pi^\pm$ and π^0. By investigating the critical points of the generating functional $\mathcal{F}$ with respect to v, m_σ and $\mathcal{M}$ we may obtain relations amongst the three variables of state

$$\frac{\partial \mathcal{F}}{\partial v}\Big|_{T,m_\sigma,\mathcal{M}} = \frac{v}{g^2}(m_\sigma^2 - 8g^2v^2) = 0, \tag{6.17}$$

$$\frac{\partial \mathcal{F}}{\partial m_\sigma}\Big|_{T,v,\mathcal{M}} = -\frac{m_\sigma}{g^2}\left(\mathcal{M}^2 - v^2 - g^2\left(J_1(T,m_\sigma) + \frac{m_\sigma^2}{16\pi^2}\ln\left[\frac{m_\sigma^2}{m_{\sigma(\mathrm{vac})}^2}\right]\right)\right) = 0, \tag{6.18}$$

$$\begin{aligned}\frac{\partial \mathcal{F}}{\partial \mathcal{M}}\Big|_{T,v,m_\sigma} = 4\mathcal{M}\Bigg(& v^2 - v_0^2 - \frac{1}{4g^2}(m_\sigma^2 - 8g^2v^2) + 3(\mathcal{M}^2 - v^2) + \frac{g_2T^2l^2}{2g^2} + \frac{\lambda_{\sigma\phi}\phi^2}{2g^2} + \\ & \frac{3}{2}\kappa(m_u + m_d)\left\{J_1(T,m_\pi) + \frac{1}{16\pi^2}m_\pi^2\ln\left[\frac{m_\pi^2}{m_{\pi(\mathrm{vac})}^2}\right]\right\}\Bigg) = 0,\end{aligned} \tag{6.19}$$

Solving the above relations respectively one obtains

$$m_\sigma(T,v)^2 = 8g^2v^2, \tag{6.20}$$

$$\begin{aligned}v^2 = v_0^2 - 3g^2&\left(J_1(T,m_\sigma) + \frac{1}{16\pi^2}m_\sigma^2\ln\left[\frac{m_\sigma^2}{m_{\sigma(\mathrm{vac})}^2}\right]\right) - \frac{\lambda\sigma\phi\ \phi^2}{2g^2} - \frac{g_2T^2l^2}{2g^2} - \\ &\frac{3}{2}\kappa(m_u + m_d)\left\{J_1(T,m_\pi) + \frac{1}{16\pi^2}m_\pi^2\ln\left[\frac{m_\pi^2}{m_{\pi(\mathrm{vac})}^2}\right]\right\}\end{aligned} \tag{6.21}$$

$$\mathcal{M}^2 = v^2 + g^2\left(J_1(T,m_\sigma) + \frac{1}{16\pi^2}m_\sigma^2\ln\left[\frac{m_\sigma^2}{m_{\sigma(\mathrm{vac})}^2}\right]\right). \tag{6.22}$$

As a result, the evolution of the σ and pion masses can be expressed in terms of temperature T and the order parameter v as $m_\sigma = m_\sigma(T,v)$ and $m_\pi \propto \mathcal{M} = \mathcal{M}(T,v)$ in accordance with equations (6.4) and (6.5). Excluding direct dependence on the meson masses allows the definition of the so-called non-equilibrium Landau functional

$$\mathcal{F}_{\mathrm{NE}}(T,v) \equiv \mathcal{F}(T,v,m_\sigma(T,v),\mathcal{M}(T,v)). \tag{6.23}$$

Further, the temperature dependence of the order parameter v may be obtained through direct use of equation (6.20). Making use of the obtained result in equation (6.23) one may define the equilibrium Landau functional as

$$\mathcal{F}_{\mathrm{E}}(T) \equiv \mathcal{F}_{\mathrm{NE}}(T,v(T)). \tag{6.24}$$

The equilibrium Landau functional $\mathcal{F}_{\mathrm{E}}$ is commonly interpreted as equivalent to the free energy of the system. This is so because the equilibrium properties of the Landau functional are analogous to those derived from the partition function in statistical mechanics [37].

The expression for the critical temperature T_c of the phase transition is obtained by solving the equality:

$$\frac{d^2\mathcal{F}_{\rm NE}}{dv^2}\Big|_{T=T_c} = 0. \tag{6.25}$$

As shown in Ref. [6] an equivalent condition may be obtained through exclusion of the order parameter v from the system of equations (6.17), (6.18) and (6.19) based on the lack of explicit dependence on the order parameter v in the terms in curly brackets. Such observation leads to relations of the form $m_\sigma(T,\mathcal{M})^2$ and $\mathcal{M}(T,m_\sigma)^2$ and motivated by graphical investigations in Ref. [6] the condition for critical temperature T_c reads:

$$\frac{dm_\sigma^2(\mathcal{M}^2)}{d\mathcal{M}^2}\Big|_{T=T_c} = \left(\frac{d\mathcal{M}^2(m_\sigma)}{dm_\sigma^2}\right)^{-1}\Big|_{T=T_c}. \tag{6.26}$$

We find the equality in equation (6.25) to be satisfied when the following relation holds:

$$\frac{8}{3}v^2\Bigg(2 - 24g^2\left[J_0(T,m_\sigma) - \frac{1}{8\pi^2}\ln\left(\frac{e\ m_\sigma^2}{m_{\sigma(\rm vac)}}\right)\right] + \tag{6.27}$$

$$3\kappa^2(m_u+m_d)^2\left[J_0(T,m_\pi) - \frac{1}{8\pi^2}\ln\left(\frac{e\ m_\pi^2}{m_{\pi(\rm vac)}}\right)\right]\left\{4g^4\left[J_0(T,m_\sigma) - \frac{1}{8\pi^2}\ln\left(\frac{e\ m_\sigma^2}{m_{\sigma(\rm vac)}}\right)\right] - 1\right\}\Bigg)$$

This relation has one-to-one correspondence with the numerator of equation (3.12) in Ref. [6], when reduced to two quark flavour case. Implying that extending the calculation presented in Ref. [6] with a constant background field has no impact on the critical temperature of the phase transition. Hence, to capture the physics of the combined model accurately, one should drop the assumption of treating the glueball field ϕ as a background field and consider it as a quantum field.

Recalling the relations between thermodynamic variables and free energy from statistical mechanics [13] we may obtain the thermal evolution of pressure $p(T)$, entropy density $\sigma(T)$, energy density $\epsilon(T)$ and heat capacity $c_V(T)$ in terms of the equilibrium Landau functional $\mathcal{F}_{\rm E}(T)$ as

$$p(T) = -\mathcal{F}_{\rm E}(T),\ \sigma(T) = -\frac{d}{dT}\mathcal{F}_{\rm E}(T),\ \epsilon(T) = \mathcal{F}_{\rm E}(T) + T\sigma,\ c_V(T) = T\frac{d\sigma}{dT} = \frac{d\epsilon}{dT}. \tag{6.28}$$

Further, using the relations between the thermodynamic variables one may also obtain the speed of sound squared

$$u^2 = \left(\frac{dp}{d\epsilon}\right)_\sigma = \frac{dp/dT}{d\epsilon/dT} = \frac{\sigma}{c_V}. \tag{6.29}$$

This is where unfortunately due to time limitations of this thesis work our investigation of extending the generating functional method presented in Ref. [6] with the glueball field ϕ and the Polyakov loop l comes to a halt. Particularly, the derivation of the analytic forms of the derivatives in equations of the thermodynamic observables and the analytic form of the equilibrium Landau functional have proven to be more involved than initially expected. This is mostly so due to the complex recursive dependence in these functions with respect to variables of state. Naively we suspect that the equations would end up reducing to the same form as presented in Ref. [6] due to the already made observation regarding the critical temperature relation. Slight straightforward extension in the case of, for example, energy-density is expected, but to fully capture the underlying physics one would need to restart the derivations in the case where also the glueball field ϕ is considered as a quantum field.

Confirmation of this assumption is left for potential future research. Once the analytic expressions of the indicated relations have been obtained one almost straightforwardly may proceed with a numerical investigation of the thermal evolution of meson masses and thermodynamic observables. One may also use a precise definition of the critical temperature entering the cosmological evolution, c.f. equation (3.7), which would account for phase transition involving both chiral symmetry breaking and confinement. This would improve the quality of the numerical results obtained in section 5. Further, one would be able to make use of the energy-density obtained from equation (6.28), rather than working in the dampened oscillator approximation as presented in equation (4.14). Combined with values of free parameters from potential future lattice simulations, one would be able to make a more accurate estimates of the relic density of DM today. Hence, most of the necessary framework for further investigations has already been laid out in the literature. The final goal would be to compare the obtained numerical results with already existing literature, where similar combinations of the models have been used.

7 CONCLUSIONS AND OUTLOOK

We have successfully combined the confining glueball field ϕ with a toy model of the LσM coupled to the Polyakov loop l, by considering two quark flavours and focusing on the gauge group $SU(3)$. We have investigated the cosmological evolution of the glueball and the σ fields as classical fields in the FRLW metric, and laid out the formalism necessary for accounting for quantum effects in the evolution through the generating functional method.

We find that, when considering the glueball ϕ and the σ fields as classical fields in a combined model, the cosmic evolution of the fields differs significantly compared to their separated evolution. Our analysis reveals that the difference between the masses of the glueball and the σ meson does not alter the evolution of the fields or the total energy density. On top of this, in our theory, the σ meson always obtains a higher mass than the glueball, when considering classical field evolution. This observation contradicts the currently phenomenological mass estimates of two mesons. However, due to lack of specific free parameter values for our theory, we have not been able to perform a thorough parameter space scan. A parameter space scan would allow us to propose physically justified mass ranges for the mesons and the relic density of our DM today.

Since the combination of the glueball, the LσM and the Polyakov loop all in one model has yet to be explored in the literature, many exciting prospects for future research are plausible. Perhaps most notably, a direct follow-up to this thesis would be completion of the generating functional method in section 6, which would describe the evolution of the glueball field ϕ and the σ field as quantum fields. Of particular interest here would be more accurately determined confinement-deconfinement critical temperature T_c, alongside thermal evolution of meson masses and thermodynamic observables describing the condensate. From the results presented in Ref. [6] we suspect that this treatment may reveal more distinct features in the behaviour of the fields as they undergo the phase transition. The QFT approach would also enable one to test the assumption laid out in Ref. [4] where it was noted that thermal effects on the cosmological evolution of the glueball field ϕ are small. To this end, one may also neglect our assumption of treating the glueball field ϕ as a spatially constant background field and consider it to be a quantum field. Since our current result for the condition of the critical temperature T_c suggest that our approach would not differ much from the ones already presented in the literature and may not accurately capture all of the underlying physics. In order to incorporate quantum corrections in the evolution one may also use alternate methods, such as, the Cornwall-Jackiw-Tomboulis method presented in the context of Polyakov loop extended LσM in Ref. [7] for investigating bubble nucleation. Further, the Polyakov loop being a non-dynamical degree of freedom neglects the mechanisms of bubble nucleation completely. As mentioned in Ref. [4] this could have a significant impact on the formation of glueballs in presence of matter fields. Accounting for this effect remains as an open question for further research.

In addition, a complete scan over the parameter space should be performed in order to determine the corresponding phase transition scale which makes the glueballs and the σ

mesons become the totality of DM. As briefly presented at the end of section 5 this may be done similarly as in Ref. [4]. However, our theory currently contains 8 free parameters on which the relic density of DM today would depend in addition to the temperature ratio between the visible and dark sectors. Hence, more constraints on the values of these parameters from lattice simulations are necessary. Moreover, one also may explore the decays, where the heavier σ meson decays into the glueball. This comes alongside a possibility for a cannibalistic phase during the evolution of either of the mesons. None of which have been investigated in this study.

Beyond that, another direct extension to this thesis work could be exchanging the toy-model utilized for incorporating the LσM and directly use the complete form of the LσM presented in equation (3.8). On top of this, a generalization of the theory to an arbitrary gauge group $SU(N)$ and arbitrary number of quark flavours N_f may take place. This would significantly increase the complexity of the problem by introducing a large number of new degrees of freedom, specifically when incorporating quantum corrections.

Lastly, the study of potential DM in the strongly coupled regime is still an ongoing field of study. Particularly, investigating other important properties this type of DM may have, and what consequences they would imply in the context of the evolution of the Universe. For strongly coupled DM to pose as a suitable candidate for DM in our Universe it has to agree with already well established experimental observations and astrophysical simulation carried out. Perhaps most notably, in the context of large structure formation in the early Universe.

8 ACKNOWLEDGEMENTS

This thesis has been possible due to time investment from a few people. First and foremost, I would like to hugely thank my supervisor Roman Pasechnik for providing invaluable guidance and exhibiting immeasurable patience through out the development of the thesis. Additionally, I would like to thank Francesco Sannino and Zhi-Wei Wang for insightful discussions regarding the surrounding physics presented in this work during our meetings. Lastly, I would like to thank my family for emotional support and allowing me to realize the dream of studying theoretical physics at an advanced level. Specifically, my grandfather who was an endless source of inspiration and strength through out my studies thus far, but unfortunately is not able to experience the completion of this work due passing away at the end stages of it.

References

[1] Piet van der Kruit. Lessons from the milky way: The kapteyn universe. 07 2014.

[2] Matthew Ho, Michelle Ntampaka, Markus Rau, Minghan Chen, Alexa Lansberry, Faith Ruehle, and Hy Trac. The dynamical mass of the coma cluster from deep learning. *Nature Astronomy*, 6:1–6, 08 2022.

[3] Vera C. Rubin and Jr. Ford, W. Kent. Rotation of the Andromeda Nebula from a Spectroscopic Survey of Emission Regions. *ApJ*, 159:379, 02 1970.

[4] Pierluca Carenza, Tassia Ferreira, Roman Pasechnik, and Zhi-Wei Wang. Glueball dark matter. *prd*, 108(12):123027, December 2023.

[5] Pierluca Carenza, Roman Pasechnik, Gustavo Salinas, and Zhi-Wei Wang. Glueball dark matter revisited. *Phys. Rev. Lett.*, 129:261302, Dec 2022.

[6] George Prokhorov and Roman Pasechnik. Light meson gas in the qcd vacuum and oscillating universe. *Journal of Cosmology and Astroparticle Physics*, 2018(01):017, jan 2018.

[7] Roman Pasechnik, Manuel Reichert, Francesco Sannino, and Zhi-Wei Wang. Gravitational waves from composite dark sectors. *JHEP*, 02:159, 2024.

[8] David Tong. Lectures on Gauge Theory. *Centre for Mathematical Sciences, Department of Applied Mathematics and Theoretical Physics, University of Cambridge*, 2018.

[9] Johan Bijnens, Lief Lönnblad, Malin Sjödahl, and Torbjörn Sjöstrand. Lecture Notes. Theoretical Particle Physics Lecture notes, 2023.

[10] Murray Gell-Mann, R. J. Oakes, and B. Renner. Behavior of current divergences under $\mathrm{su}_3 \times \mathrm{su}_3$. *Phys. Rev.*, 175:2195–2199, Nov 1968.

[11] J. Beringer, et al. Review of particle physics. *Phys. Rev. D*, 86:010001, Jul 2012.

[12] T. Schäfer and E. V. Shuryak. Instantons in qcd. *Reviews of Modern Physics*, 70(2):323–425, April 1998.

[13] David Chandler. *Introduction to Modern Statistial Mechanics*. Oxford University Press, 1987.

[14] Roman Pasechnik and Michal Šumbera. Different Faces of Confinement. *Universe*, 7(9):330, 2021.

[15] Wolfgang Ochs. The status of glueballs. *Journal of Physics G Nuclear and Particle Physics*, 40, 01 2013.

[16] Vincent Mathieu, Nikolai Kochelev, and Vicente Vento. The Physics of Glueballs. *Int. J. Mod. Phys. E*, 18:1–49, 2009.

[17] David Curtin, Caleb Gemmell, and Christopher B. Verhaaren. Simulating glueball production in $N_f = 0$ qcd. *Phys. Rev. D*, 106:075015, Oct 2022.

[18] B. Andersson, G. Gustafson, and T. Sjöstrand. A model for baryon production in quark and gluon jets. *Nuclear Physics B*, 197(1):45–54, 1982.

[19] Benjamin Svetitsky and Laurence G. Yaffe. Critical behavior at finite-temperature confinement transitions. *Nuclear Physics B*, 210(4):423–447, 1982.

[20] Francesco Sannino. Polyakov loops versus hadronic states. *Phys. Rev. D*, 66:034013, Aug 2002.

[21] Wei-Chih Huang, Manuel Reichert, Francesco Sannino, and Zhi-Wei Wang. Testing the dark su(n) yang-mills theory confined landscape: From the lattice to gravitational waves. *Phys. Rev. D*, 104:035005, Aug 2021.

[22] Lindsay Forestell, David E. Morrissey, and Kris Sigurdson. Non-abelian dark forces and the relic densities of dark glueballs. *Phys. Rev. D*, 95:015032, Jan 2017.

[23] Biagio Lucini, Antonio Rago, and Enrico Rinaldi. Su(nc) gauge theories at deconfinement. *Physics Letters B*, 712(3):279–283, 2012.

[24] Mara Grahl and Dirk H. Rischke. Functional renormalization group study of the two-flavor linear sigma model in the presence of the axial anomaly. *Phys. Rev. D*, 88(5):056014, 2013.

[25] Y. Meurice. Linear sigma model for multiflavor gauge theories. *Phys. Rev. D*, 96:114507, Dec 2017.

[26] Tetsuya Akutagawa, Koji Hashimoto, Takeshi Miyazaki, and Toshihiro Ota. Phase diagram of qcd chaos in linear sigma models and holography. *Progress of Theoretical and Experimental Physics*, 2018, 04 2018.

[27] Alexey A. Petrov. Glueball-meson molecules. *Physics Letters B*, 843:138030, 2023.

[28] Denis Parganlija, Francesco Giacosa, and Dirk H. Rischke. Vacuum properties of mesons in a linear sigma model with vector mesons and global chiral invariance. *Physical Review D*, 82(5), September 2010.

[29] D. Parganlija, P. Kovács, Gy. Wolf, F. Giacosa, and D. H. Rischke. Meson vacuum phenomenology in a three-flavor linear sigma model with (axial-)vector mesons. *Phys. Rev. D*, 87:014011, Jan 2013.

[30] Stanislaus Janowski, Denis Parganlija, Francesco Giacosa, and Dirk Rischke. The glueball in a chiral linear sigma model with vector mesons. *Physical Review D - PHYS REV D*, 84, 03 2011.

[31] Eric D. Carlson, Marie E. Machacek, and Lawrence J. Hall. Self-interacting Dark Matter. *apj*, 398:43, oct 1992.

[32] Kenji Fukushima and Vladimir Skokov. Polyakov loop modeling for hot qcd. *Progress in Particle and Nuclear Physics*, 96:154–199, 2017.

[33] Ágnes Mócsy, Francesco Sannino, and Kimmo Tuominen. Confinement versus chiral symmetry. *Phys. Rev. Lett.*, 92:182302, May 2004.

[34] Dimitry Gorbunov and Valery Rubakov. *Introduction to the Theory of the Early Universe, Hot Big Bang Theory, Second Edition.* World Scientific Publishing Co, Pte. Ltd., 2017.

[35] G. W. Carter, O. Scavenius, I. N. Mishustin, and P. J. Ellis. Effective model for hot gluodynamics. *Phys. Rev. C*, 61:045206, Mar 2000.

[36] E. S. Bowman. Linear Sigma Model at Finite Temperature and Chemical Potentials. Other thesis, Uppsala universitet, 5 2010.

[37] Peter Olmsted. Lectures on Landau Theory of Phase Transitions. Department of Physics, Georgetown University, 2015.